

This is a pre print version of the following article:

Solution structure of a pentachromium(II) single molecule magnet from DFT calculations, isotopic labelling and multinuclear NMR spectroscopy / Dirvanauskas, Aivaras; Galavotti, Rita; Lunghi, Alessandro; Nicolini, Alessio; Roncaglia, Fabrizio; Totti, Federico; Cornia, Andrea. - In: DALTON TRANSACTIONS. - ISSN 1477-9226. - 47:2(2018), pp. 585-595. [10.1039/c7dt03931j]

*Terms of use:*

The terms and conditions for the reuse of this version of the manuscript are specified in the publishing policy. For all terms of use and more information see the publisher's website.

19/12/2025 03:02



**Solution Structure of a Pentachromium(II) Single Molecule  
Magnet from Isotopic Labelling and Multinuclear NMR  
Spectroscopy**

Journal:	<i>Dalton Transactions</i>
Manuscript ID	Draft
Article Type:	Paper
Date Submitted by the Author:	n/a
Complete List of Authors:	Dirvanauskas, Aivaras; University of Modena and Reggio Emilia, Department of Chemical and Geological Sciences; University of Warwick, Department of Chemistry Galavotti, Rita; University of Modena and Reggio Emilia, Department of Chemical and Geological Sciences Lunghi, Alessandro; University of Florence, Chemistry Nicolini, Alessio; University of Modena and Reggio Emilia, Department of Chemical and Geological Sciences Roncaglia, Fabrizio; University of Modena and Reggio Emilia, Department of Chemical and Geological Sciences Totti, Federico; University of Florence, Chemistry Cornia, Andrea; University of Modena and Reggio Emilia, Department of Chemical and Geological Sciences



UNIMORE  
UNIVERSITÀ DEGLI STUDI DI  
MODENA E REGGIO EMILIA

DIPARTIMENTO DI SCIENZE CHIMICHE E GEOLOGICHE

Modena, October 18, 2017

Dear Editor of *Dalton Transactions*,

I enclose the original manuscript entitled “**Solution Structure of a Pentachromium(II) Single Molecule Magnet from Isotopic Labelling and Multinuclear NMR Spectroscopy**” by Dirvanauskas *et al.*, which I submit on an exclusive basis to your journal as a full article, with the consent of all coauthors. The paper tackles for the first time the much debated structure of pentachromium(II) Extended Metal Atom Chain  $[\text{Cr}_5(\text{tpda})_4\text{Cl}_2]$  by applying DFT calculations as well as high-resolution proton and deuteron liquid-phase NMR spectroscopies on native and isotopically-enriched samples. Understanding the structure of these highly conducting “molecular wires” in the absence of the rigid constraints of a crystal lattice is deemed important to correctly approach their electron transport properties, which have been reported in recent papers (see refs. 4 and 12).

The main focus of our manuscript is on the structural properties as revealed by DFT calculations and spectroscopic studies. However, the text also details a new, high-yield procedure for the preparation of  $\text{H}_2\text{tpda}$  ligand, which may be of great interest for research groups working on string-like complexes of oligo- $\alpha$ -aminopyridines. As a considerable aid in spectroscopic work, we also describe routes for post-synthetic isotopic labelling of  $\text{H}_2\text{tpda}$ , which might be easily extended to other ligands of the same class.

Thus, I strongly believe that our manuscript will be attractive and useful for the broad inorganic and organometallic readership of *Dalton Transactions* interested in coordination complexes for molecular electronics and neighboring fields.

With the hope that you will appreciate the originality, relevance, and quality of our investigation, I thank you for your kind attention.

Best regards,

Andrea Cornia

Submitting author on behalf of all coauthors

---

Sede Legale: Via G. Campi, 103 – 41125 Modena

Direzione: Tel.: 059 205 8518 - e-mail: [direttore.chimgeo@unimore.it](mailto:direttore.chimgeo@unimore.it)

Amministrazione: Tel.: 059 205 8521 – indirizzo istituzionale e-mail: [segreteria.chimgeo@unimore.it](mailto:segreteria.chimgeo@unimore.it)

e-mail PEC: [giuseppegb.chimgeo@pec.unimore.it](mailto:giuseppegb.chimgeo@pec.unimore.it)

Partita IVA.: 00427620364  
Codice IPA: FZY9SO

per Creditori Privati: Conto Unicredit: IT40H0200812930000102063651 – SWIFT CODE: UNCRITMM - Codice Bilancio UNIMORE: 1005

per Creditori Pubblici: Conto Banca d'Italia: IT23E0100003245243300037150

# Solution Structure of a Pentachromium(II) Single Molecule Magnet from Isotopic Labelling and Multinuclear NMR Spectroscopy†

Aivaras Dirvanauskas,<sup>a,b</sup> Rita Galavotti,<sup>a</sup> Alessandro Lunghi,<sup>‡c</sup> Alessio Nicolini,<sup>a</sup> Fabrizio Roncaglia,<sup>a</sup> Federico Totti<sup>c</sup> and Andrea Cornia<sup>a\*</sup>

<sup>a</sup>*Department of Chemical and Geological Sciences, University of Modena and Reggio Emilia & INSTM, I-41125 Modena, Italy*

<sup>b</sup>*Department of Chemistry, University of Warwick, Gibbet Hill, Coventry, CV4 7AL, United Kingdom*

<sup>c</sup>*Department of Chemistry ‘Ugo Schiff’, University of Florence & INSTM, I-50019 Sesto Fiorentino (FI), Italy*

**Abstract.** The structure of pentachromium(II) Extended Metal Atom Chain [Cr<sub>5</sub>(tpda)<sub>4</sub>Cl<sub>2</sub>] (**2**), which behaves as a Single Molecule Magnet at low temperature, was investigated by Density Functional Theory (DFT) calculations and spectroscopic studies without the constraints of a crystal lattice (H<sub>2</sub>tpda = *N*<sup>2</sup>,*N*<sup>6</sup>-bis(pyridin-2-yl)pyridine-2,6-diamine). DFT studies both in the gas phase and including CH<sub>2</sub>Cl<sub>2</sub> solvent effects indicate that an unsymmetric structure (*C*<sub>4</sub> point group), with pairs of formally quadruply-bonded metal ions and one terminal metal center, is slightly more stable (2.9 and 3.9 kcal/mol) than a symmetric structure (*D*<sub>4</sub> point group). Isotopically-labelled samples (**2**-*d*<sub>8</sub> and **2**-*d*<sub>16</sub>) have then been prepared to aid in molecular symmetry determination by combined <sup>1</sup>H and <sup>2</sup>H NMR studies in CH<sub>2</sub>Cl<sub>2</sub> solution. The spectra are strongly suggestive of a symmetric (*D*<sub>4</sub>) framework, indicating fast shuttling between the two unsymmetric forms over the timescale of NMR experiments. Procedures for a high-yield Pd-free synthesis of H<sub>2</sub>tpda and for site-selective post-synthetic H/D exchange of aromatic H<sub>2</sub>tpda hydrogens are also reported.

†Electronic Supplementary Information (ESI) available: chemical scheme on the reactivity of mixtures of 2,6-dibromopyridine and 2,6-diaminopyridine (Fig. S1), scale-expanded proton NMR spectra of H<sub>2</sub>tpda, H<sub>2</sub>tpda-*d*<sub>2</sub>, and H<sub>2</sub>tpda-*d*<sub>4</sub> (Fig. S2), proton NMR spectrum of H<sub>2</sub>tpda-*d*<sub>2</sub> obtained by acidic H/D exchange (Fig. S3 and S4), full-range ESI-MS spectra of **2**, **2**-*d*<sub>8</sub> and **2**-*d*<sub>16</sub> (Fig. S5). For ESI see DOI: XXXXXX.

‡Current address: School of Physics, AMBER and CRANN, Trinity College, Dublin 2, Ireland.

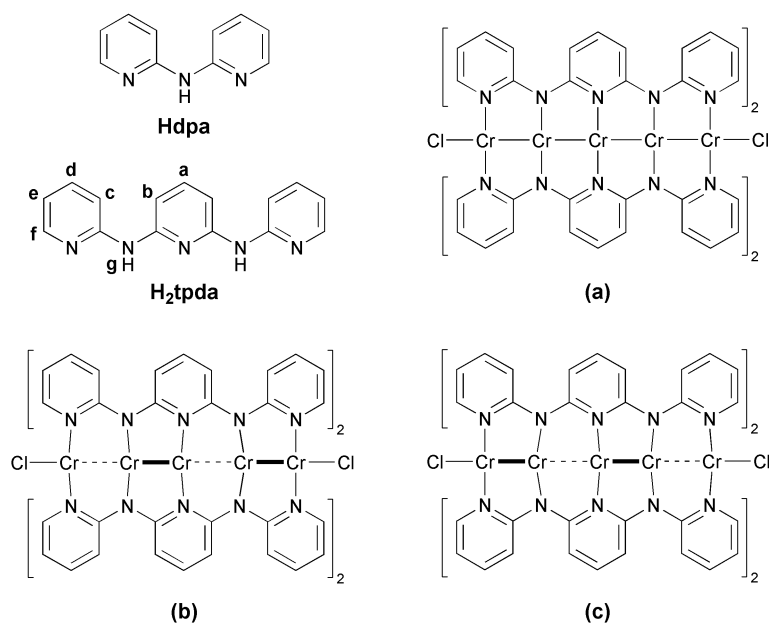
## Introduction

One-dimensional molecular complexes containing metal-metal bonds are attractive both as simple benchmark systems for studying metal-metal interactions and as prototypical molecular wires with a prominent application potential in nanoelectronics.<sup>1-4</sup> Among viable synthetic strategies to assemble linear arrays of mutually-bonded metal atoms,<sup>5</sup> properly-designed organic ligands are often used to enforce sufficiently short metal-metal distances, so that direct overlap of *d* orbitals occurs. Many of these complexes, known since 2003 as Extended Metal Atom Chains (EMACs),<sup>6-9</sup> comprise oligo- $\alpha$ -aminopyridines or related ligands that contain *N*-based heterocycles.<sup>10</sup> The fully-deprotonated, all-*syn* conformation of these ligands can form a helical coil and wrap around strings of up to eleven metal ions.<sup>11,12</sup> This ligand geometry is efficient in promoting formation of metal-metal bonds, but the exact pattern of metal-metal distances and the extent of bond delocalization have represented a much debated issue. Especially controversial is the interpretation of crystallographic data for tri- and pentachromium(II) derivatives [Cr<sub>3</sub>(dpa)<sub>4</sub>Cl<sub>2</sub>] (**1**) and [Cr<sub>5</sub>(tpda)<sub>4</sub>Cl<sub>2</sub>] (**2**) (see Scheme 1), which both behave as Single Molecule Magnets at low temperature (Hdpa = *N*-(pyridin-2-yl)pyridin-2-amine,<sup>13</sup> H<sub>2</sub>tpda = *N*<sup>2</sup>,*N*<sup>6</sup>-bis(pyridin-2-yl)pyridine-2,6-diamine).<sup>14,15</sup> The solid-state structures of these EMACs often show metal atoms with abnormally elongated (prolate) displacement ellipsoids along the chain axis, which can be interpreted as due to either large thermal vibrations or to positional disorder effects. The first model results in approximately equal metal-metal distances along the chain (Scheme 1a), which hint to electronic delocalization.<sup>16,17</sup> On the other hand, the assumption of static disorder (“split-atom” model) affords an alternation of short (*d*<sub><</sub>) and long (*d*<sub>></sub>) distances (Scheme 1b,c), suggesting dimerization into pairs of quadruply-bonded chromium(II) ions.<sup>18-21</sup> This structural asymmetry, evaluated as  $\Delta d = d_{>} - d_{<}$ , ranges from 0.22 to 0.26 Å in solvatomorphs of **1** at –60°C.<sup>18</sup> However, an illuminating structural study by Wu *et al.* has cast serious doubts on the validity of a “split-atom” model for the trichromium(II) string in **1**·Et<sub>2</sub>O. At 15 K, this molecule adopts a symmetric structure in the solid state, with no evidence for static disorder.<sup>22</sup> These results are in complete agreement with Density Functional Theory (DFT) calculations, which indicate a symmetric gas-phase equilibrium structure for **1**<sup>23</sup> and its congeners, except for those containing very weak axial ligands (*e.g.* NO<sub>3</sub><sup>–</sup>).<sup>24</sup> However, the central metal ion lies in a very shallow potential energy surface and distortion of the symmetric structure is an energetically facile process, thereby explaining the structural versatility of trichromium(II) strings.<sup>18,25,26</sup> In pentachromium(II) EMACs, as well as in their Cr<sub>7</sub> and Cr<sub>9</sub> congeners,<sup>27,28</sup> application of the “split-atom” model results in a much more pronounced structural asymmetry, with *d*<sub><</sub> = 1.86-2.03 Å, *d*<sub>></sub> = 2.58-2.66 Å and  $\Delta d \sim 0.7$  Å in solvatomorphs of **2** at –60°C.<sup>19,20</sup> These complexes seemingly feature quadruply-bonded Cr<sub>2</sub><sup>4+</sup> units *plus* one terminal high-spin (*S* = 2)

chromium(II) center, that in **2** exhibits a directionally-bistable magnetic moment and is at the origin of the observed SMM behaviour.<sup>15</sup>

Structural information on chromium-based EMACs without the rigid constraints of a crystal lattice is comparatively scarce,<sup>29,30</sup> although such studies are of importance to the field of single-molecule electronics. Within the series  $[M_n(L)_4(SCN)_2]$  ( $M = Co, Ni$  for  $n = 3, 5$ ;  $M = Cr$  for  $n = 3, 5, 7$ ;  $L =$  oligo- $\alpha$ -pyridylamide) the Cr derivatives are especially interesting in that they displays the highest single-molecule conductance among strings of the same length.<sup>4</sup>

We have now performed DFT calculations and found that, at variance with its trichromium(II) congener **1**, complex **2** has an unsymmetric ground structure, although in the gas phase the symmetric form lies only 2.9 kcal mol<sup>-1</sup> higher in energy. Such an energy difference becomes 3.9 kcal mol<sup>-1</sup> when implicit solvent effects (CH<sub>2</sub>Cl<sub>2</sub>) are included. Next, we have used NMR methods and an isotopic labelling strategy to investigate the structure adopted by **2** in solution. To simplify the spectra and aid in peak assignment, we have first developed an improved Pd-free route to bulk quantities of H<sub>2</sub>tpda (Scheme 1). Subsequently we have carried out post-synthetic isotopic labelling with deuterium on *b* positions only (H<sub>2</sub>tpda-*d*<sub>2</sub>) or on both *b* and *f* positions (H<sub>2</sub>tpda-*d*<sub>4</sub>). <sup>1</sup>H-NMR spectroscopy has then been complemented with <sup>2</sup>H-NMR on samples of **2**, [Cr<sub>5</sub>(tpda-*d*<sub>2</sub>)<sub>4</sub>Cl<sub>2</sub>] (**2-d**<sub>8</sub>) and [Cr<sub>5</sub>(tpda-*d*<sub>4</sub>)<sub>4</sub>Cl<sub>2</sub>] (**2-d**<sub>16</sub>) in CH<sub>2</sub>Cl<sub>2</sub> solution. The results provide clear evidence that this pentachromium(II) complex has a symmetric (*D*<sub>4</sub>) structure, meaning that it shuttles between the two unsymmetric forms at a rate faster than NMR timescale.



**Scheme 1.** Hdpa and H<sub>2</sub>tpda ligands (with the hydrogen labelling scheme), and [Cr<sub>5</sub>(tpda)<sub>4</sub>Cl<sub>2</sub>] (**2**) complex in its symmetric (a) and unsymmetric (b,c) structures.

## Experimental

### General procedures

Chemicals were of reagent grade and were used as received, unless otherwise noted. D<sub>2</sub>O (99.97 D%) and CD<sub>3</sub>OD (99.8 D%) were used for H/D exchange experiments. All operations involving chromium(II) complexes were carried out inside an MBraun UniLAB glovebox using anhydrous solvents degassed by three freeze-pump-thaw cycles. Room temperature <sup>1</sup>H and <sup>2</sup>H NMR spectra were recorded at 400.13 and 61.42 MHz, respectively, on a Bruker Avance400 FT-NMR spectrometer. Proton chemical shifts are expressed in ppm downfield from Me<sub>4</sub>Si as external standard, by setting the residual <sup>1</sup>H signal of DMSO-*d*<sub>6</sub> and CD<sub>2</sub>Cl<sub>2</sub> at 2.50 and 5.32 ppm, respectively.<sup>31</sup> The chemical shift (ppm) axis in <sup>2</sup>H spectra was calibrated by setting the deuterium signal of DMSO and CH<sub>2</sub>Cl<sub>2</sub> at 2.50 and 5.32 ppm, respectively. Spectra analysis was carried out with TopSpin 3.5 pl 7 software using the following processing parameters: SI = TD, LB = 0.05 (0.3) Hz for <sup>1</sup>H (<sup>2</sup>H) spectra of the ligands, LB = 0.5 Hz for both <sup>1</sup>H and <sup>2</sup>H spectra of the complexes. *J* values are given in Hz. Isotopic enrichments were evaluated from proton spectra by setting the integrated area of *He* signal equal to 2*H*. The intensity of this peak was always larger or equal to that of the remaining signals (with the obvious exception of *Ha*), indicating a negligible tendency of *He* protons to undergo H/D exchange in the explored conditions. Spectra of **2**, **2-*d*<sub>8</sub>** and **2-*d*<sub>16</sub>** complexes were recorded in valved 5-mm NMR tubes loaded inside the above mentioned glovebox (ca. 8-10 mg in 0.9-1.0 mL of solvent). In the case of **2-*d*<sub>8</sub>** and **2-*d*<sub>16</sub>** <sup>2</sup>H spectra in CH<sub>2</sub>Cl<sub>2</sub> were first recorded, then the solvent was completely evaporated and the solid residue redissolved in CD<sub>2</sub>Cl<sub>2</sub> for measuring <sup>1</sup>H spectra. ESI-MS measurements were made in positive ion mode on an Agilent Technologies 6310A Ion Trap LC-MS(n) instrument by direct infusion of solutions in anhydrous and deoxygenated CH<sub>2</sub>Cl<sub>2</sub>. Isotopic patterns were simulated using Isotope Distribution Calculator.<sup>32</sup>

### Synthesis and H/D exchange

**H<sub>2</sub>tpda.** 2,6-Diaminopyridine (0.546 g, 5.0 mmol) and LiH (0.270 g, 34 mmol) were sequentially introduced in a 50 mL round bottomed flask under Ar and stirred for 5 min. A small condenser topped by a CaCl<sub>2</sub> tube was mounted and flushed with Ar, then 2-fluoropyridine (1.3 mL, 1.47 g, 15.1 mmol) and pyridine (2.6 mL) were added from the top using a pipette. After 5 minutes, the flask was immersed in an oil bath preheated at 150°C and some minutes later (before the mixture became a solid mass) toluene (7.0 mL) was introduced. The mixture was stirred for 3 h and 15 min and then cooled down with a water bath. TLC (eluent CH<sub>2</sub>Cl<sub>2</sub>:EtOH 9:1 + 3 drops of 30% aqueous ammonia) showed no 2,6-diaminopyridine (r.f. 0.34), traces of dimer **A** (see Scheme 2, r.f. 0.49)

and a substantial amount of H<sub>2</sub>tpda (r.f. 0.68). Solvent was removed under vacuum, water (40 mL) was added to the solid residue and the mixture was stirred for 10 min. Filtration through a Gooch funnel (porosity no. 3) followed by extensive washing (3 × 15 mL water + 2 × 20 mL hot water) afforded a wet beige solid. This was dissolved in THF (45 mL) and filtered on a short silica plug (1.0 g), which was washed with fresh THF (2 × 5 mL). Removal of all volatiles from the combined THF phases gave H<sub>2</sub>tpda as a brownish solid (1.25 g, 95%) with excellent TLC purity. To gain further purification a practical digestion method was developed. In a 25 mL round bottom flask containing crude H<sub>2</sub>tpda (1.25 g, 4.75 mmol), CH<sub>3</sub>OH (5 mL), CH<sub>2</sub>Cl<sub>2</sub> (5 mL) and Et<sub>2</sub>O (5 mL) were added and the mixture left in agitation for 3 h at r.t.. The flask was cooled in an ice bath, then the mixture was filtered through a Gooch funnel (porosity no. 3) and the collected solid washed with Et<sub>2</sub>O (3 × 2 mL). After drying at a mechanical pump, purified H<sub>2</sub>tpda was obtained (1.18 g, 94%, 90% overall) as a beige solid. mp 222°C.  $\delta$ H (400 MHz; DMSO-*d*<sub>6</sub>; Me<sub>4</sub>Si) 9.37 (2H, s, Hg), 8.21 (2H, ddd,  $^3J(f,e) = 4.9$ ,  $^4J(f,d) = 1.9$ ,  $^5J(f,c) = 0.8$ , Hf), 7.83 (2H, ddd,  $^3J(c,d) = 8.5$ ,  $^4J(c,e) \sim ^5J(c,f) \sim 0.9$ , Hc), 7.64 (2H, ddd,  $^3J(d,c) = 8.5$ ,  $^3J(d,e) = 7.1$ ,  $^4J(d,f) = 1.9$ , Hd), 7.50 (1H, t,  $^3J(a,b) = 8.0$ , Ha), 7.13 (2H, d,  $^3J(b,a) = 8.0$ , Hb), 6.85 (2H, ddd,  $^3J(e,d) = 7.1$ ,  $^3J(e,f) = 4.9$ ,  $^4J(e,c) = 1.0$ , He).

**H<sub>2</sub>tpda-*d*<sub>2</sub>**. H<sub>2</sub>tpda (100 mg) and D<sub>2</sub>O (1.55 mL) were introduced in a 2 mL stainless steel vessel and the screw cap closed. The vessel was placed in a preheated oven at 220°C for 24 h. After cooling, the yellowish-green solid material was recovered and washed with water (5 mL) to give a beige solid (83 mg, 82%).  $^1$ H NMR analysis indicated 90.5% and 15.5% deuteration on *b* and *f* positions, respectively. Although Hc and Hd occur in two different environments, due to the small percentage of deuteration on *f* positions the minority component was difficult to resolve and was neglected in the assignments below.  $\delta$ H (400 MHz; DMSO-*d*<sub>6</sub>; Me<sub>4</sub>Si) 9.36 (2H, s, Hg), 8.21 (1.69H, ddd,  $^3J(f,e) = 4.9$ ,  $^4J(f,d) = 1.9$ ,  $^5J(f,c) = 0.8$ , Hf), 7.83 (2H, ddd,  $^3J(c,d) = 8.4$ ,  $^4J(c,e) \sim ^5J(c,f) \sim 0.9$ , Hc), 7.64 (2H, ddd,  $^3J(d,c) = 8.4$ ,  $^3J(d,e) = 7.2$ ,  $^4J(d,f) = 1.9$ , Hd), 7.50 (0.19H, d,  $^3J(a,b) = 8.0$ , Ha in molecules with one residual Hb), 7.50 (0.81H, s, Ha in molecules with no residual Hb), 7.13 (0.19H, d,  $^3J(b,a) = 8.0$ , Hb), 6.85 (1.69H, ddd,  $^3J(e,d) = 7.2$ ,  $^3J(e,f) = 4.9$ ,  $^4J(e,c) = 1.0$ , He in pyridyl groups not deuterated on *f* position), 6.85 (0.31H, dd,  $^3J(e,d) = 7.1$ ,  $^4J(e,c) = 1.0$ , He in pyridyl groups deuterated on *f* position).

**H<sub>2</sub>tpda-*d*<sub>2</sub>** (by acidic H/D exchange). D<sub>2</sub>O (5.0 mL) was introduced in a test tube equipped with a ground joint and a septum. After cooling in an ice bath, distilled AcCl (1.0 mL, 1.1 g, 14 mmol) was added through the septum under stirring, the solution was allowed to warm up to room temperature and H<sub>2</sub>tpda (50 mg, 0.21 mmol) was added to give a yellow solution. A condenser was mounted on top of the test tube and the solution was refluxed, with regular sampling (1.0 mL) every



hour. The work up of each sampled fraction consisted in adding solid NaOH (ca. 0.3 g) until alkaline pH. The beige precipitate was filtered out, washed with water (1.0 mL) and Et<sub>2</sub>O (1.0 mL) and dissolved in hot THF (1.5 mL). Removal of all volatiles in vacuo afforded a yellowish solid (total: 48 mg, 95%). <sup>1</sup>H NMR analysis indicated a high degree of deuteration of *b* positions (96.7 %) already after 2 h of reflux, with negligible H/D exchange on the remaining positions; after 4 h a further increase of isotopic enrichment at *b* positions (98.1%) was accompanied by the onset of deuteration (few percent) of the remaining protons.  $\delta$ H (400 MHz; DMSO-*d*<sub>6</sub>; Me<sub>4</sub>Si) 9.36 (2H, s, Hg), 8.21 (2H, ddd, <sup>3</sup>*J*(*f*,*e*) = 4.9, <sup>4</sup>*J*(*f*,*d*) = 1.9, <sup>5</sup>*J*(*f*,*c*) = 0.8, Hf), 7.82 (2H, ddd, <sup>3</sup>*J*(*c*,*d*) = 8.5, <sup>4</sup>*J*(*c*,*e*) ~ <sup>5</sup>*J*(*c*,*f*) ~ 0.9, Hc), 7.63 (2H, ddd, <sup>3</sup>*J*(*d*,*c*) = 8.5, <sup>3</sup>*J*(*d*,*e*) = 7.1, <sup>4</sup>*J*(*d*,*f*) = 1.9, Hd), 7.50 (0.065H, d, <sup>3</sup>*J*(*a*,*b*) = 8.0, Ha in molecules with one residual Hb), 7.50 (0.935H, s, Ha in molecules with no residual Hb), 7.12 (0.065H, d, <sup>3</sup>*J*(*b*,*a*) = 8.0, Hb), 6.85 (2H, ddd, <sup>3</sup>*J*(*e*,*d*) = 7.1, <sup>3</sup>*J*(*e*,*f*) = 4.9, <sup>4</sup>*J*(*e*,*c*) = 1.0, He).

**H<sub>2</sub>tpda-*d*<sub>4</sub>.** H<sub>2</sub>tpda (56 mg), CD<sub>3</sub>OD (0.1 mL) and D<sub>2</sub>O (1.75 mL) were introduced in a 2 mL stainless steel vessel and the screw cap closed. The vessel was placed in a preheated oven at 230°C for 24 h. The same work-up described for **H<sub>2</sub>tpda-*d*<sub>2</sub>** gave a beige solid (35 mg, 62%). <sup>1</sup>H NMR analysis indicated 98%, 83% and 4% deuteration on *b*, *f* and *c* positions, respectively. Three additional runs gave: 98% (*b*), 80% (*f*), 3% (*c*); 98% (*b*), 69% (*f*), 3% (*c*); 96% (*b*), 63% (*f*), 1% (*c*). 12.5-, 26.0-, 29.0- and 20.8-mg samples of deuterated H<sub>2</sub>tpda from these four batches, respectively, were combined and used in subsequent reactions. The effect of partial deuteration of *c* positions on Hf and He resonances, as well as of residual Hf protons on Hc, Hd and He resonances could not be resolved and was neglected in the assignments below.  $\delta$ H (400 MHz; DMSO-*d*<sub>6</sub>; Me<sub>4</sub>Si) 9.36 (2H, s, Hg), 8.21 (0.34H, ddd, <sup>3</sup>*J*(*f*,*e*) = 4.9, <sup>4</sup>*J*(*f*,*d*) = 1.9, <sup>5</sup>*J*(*f*,*c*) = 0.8, Hf), 7.83 (1.91H, dd, <sup>3</sup>*J*(*c*,*d*) = 8.4, <sup>4</sup>*J*(*c*,*e*) = 0.9, Hc), 7.64 (1.91H, dd, <sup>3</sup>*J*(*d*,*c*) = 8.4, <sup>3</sup>*J*(*d*,*e*) = 7.2, Hd in pyridyl groups not deuterated on *c* position), 7.64 (0.09H, d, <sup>3</sup>*J*(*d*,*e*) = 7.2, Hd in pyridyl groups deuterated on *c* position), 7.50 (0.034H, d, <sup>3</sup>*J*(*a*,*b*) = 8.0, Ha in molecules with one residual Hb), 7.50 (0.966H, s, Ha in molecules with no residual Hb), 7.13 (0.034H, d, <sup>3</sup>*J*(*b*,*a*) = 8.0, Hb), 6.85 (2H, dd, <sup>3</sup>*J*(*e*,*d*) = 7.2, <sup>4</sup>*J*(*e*,*c*) = 0.9, He).  $\delta$ D (61 MHz; DMSO; see above) 8.2 (2D, br s, Df), 7.1 (2D, br s, Db).

**[Cr<sub>5</sub>(tpda)<sub>4</sub>Cl<sub>2</sub>] $\cdot$ 4CHCl<sub>3</sub> $\cdot$ 2Et<sub>2</sub>O (2 $\cdot$ 4CHCl<sub>3</sub> $\cdot$ 2Et<sub>2</sub>O).** The compound was prepared using the procedure described by Chang *et al.*<sup>15,17</sup>  $\delta$ H (400 MHz; CD<sub>2</sub>Cl<sub>2</sub>; Me<sub>4</sub>Si) 13.0 (br), 2.3 (br), 1.0 (br), 0.1 (br), -10.2 (br). ESI-MS: *m/z* 1376.2 ([Cr<sub>5</sub>(tpda)<sub>4</sub>Cl<sub>2</sub>]<sup>+</sup>, 100%), 1359.2 (4.11).

**[Cr<sub>5</sub>(tpda-*d*<sub>2</sub>)<sub>4</sub>Cl<sub>2</sub>] $\cdot$ 4CHCl<sub>3</sub> $\cdot$ 2Et<sub>2</sub>O (2-*d*<sub>8</sub> $\cdot$ 4CHCl<sub>3</sub> $\cdot$ 2Et<sub>2</sub>O).** H<sub>2</sub>tpda-*d*<sub>2</sub> obtained by H/D exchange in D<sub>2</sub>O (81 mg, 0.31 mmol), CD<sub>3</sub>OD (1.3 mL) and THF (2.0 mL) were introduced in a conical flask. The mixture was heated to reflux until complete dissolution, then naphthalene (2.0 g) was added and the mixture heated to 100°C for 1 h to evaporate all volatiles. The flask was then cooled down

to room temperature and  $\text{CrCl}_2$  (58 mg, 0.47 mmol) and  $t\text{BuOK}$  (69 mg, 0.61 mmol) were added. The procedure for the reaction and the subsequent workup and crystallization were identical to those previously described for the nondeuterated analogue and the yield was comparable ( $\sim 30\%$ ).<sup>15,17</sup>  $\delta\text{H}$  (400 MHz;  $\text{CD}_2\text{Cl}_2$ ;  $\text{Me}_4\text{Si}$ ) 13.0 (br), 2.3 (br), 0.1 (br),  $-10.2$  (br).  $\delta\text{D}$  (61 MHz;  $\text{CH}_2\text{Cl}_2$ ; see above) 0.85 (br). ESI-MS:  $m/z$  1383.1 ( $[\text{Cr}_5(\text{tpda-}d_2)_4\text{Cl}_2]^+$ , 100%), 1366.1 (0.73).

**$[\text{Cr}_5(\text{tpda-}d_4)_4\text{Cl}_2] \cdot 4\text{CHCl}_3 \cdot 2\text{Et}_2\text{O}$  ( $2\text{-}d_{16} \cdot 4\text{CHCl}_3 \cdot 2\text{Et}_2\text{O}$ ).** The synthesis also followed the above-described procedure, using:  $\text{H}_2\text{tpda-}d_4$  (88 mg, 0.33 mmol) from four different batches, with average isotopic enrichment 97.5% (*b*), 72.8% (*f*), 2.7% (*c*);  $\text{CD}_3\text{OD}$  (1.5 mL), THF (2 mL), naphthalene (2.0 g),  $\text{CrCl}_2$  (63 mg, 0.51 mmol) and  $t\text{BuOK}$  (76 mg, 0.68 mmol). The yield was comparable ( $\sim 30\%$ ).<sup>15,17</sup>  $\delta\text{H}$  (400 MHz;  $\text{CD}_2\text{Cl}_2$ ;  $\text{Me}_4\text{Si}$ ) 13.0 (br), 2.4 (br), 0.1 (br),  $-10.2$  (br).  $\delta\text{D}$  (61 MHz;  $\text{CH}_2\text{Cl}_2$ ; see above) 0.82 (br). ESI-MS:  $m/z$  1389.2 ( $[\text{Cr}_5(\text{tpda-}d_4)_4\text{Cl}_2]^+$ , 100%), 1371.2 (2.79).

## Density Functional Theory (DFT) Calculations

DFT calculations were performed with the ORCA program package, version 3.0.3.<sup>33</sup> Optimized geometries were computed using the PBE functional.<sup>34</sup> D3 dispersion corrections scheme<sup>35</sup> was also used. Scalar relativistically recontracted versions of the Ahlrichs triple- $\zeta$  basis set, def2-TZVP, were used on Cr, N, and Cl atoms while single- $\zeta$  basis set, def2-SVP, was used for C and H atoms.<sup>36,37</sup> The conductor-like screening model (COSMO)<sup>38</sup> was used to simulate a  $\text{CH}_2\text{Cl}_2$  solution ( $\epsilon = 9.08$ ). The reason for performing the geometry optimizations within a model solvent was to exclude any solvent effect in the localization/delocalization of the Cr-Cr bonds. Resolution of identity (RI) was used to approximate two electron integrals. Considered that **2** spans a very flat potential energy surface, two different starting geometries were chosen: symmetric and unsymmetric arrangements of the Cr atoms. A tight convergence threshold was also used (TightOpt). The SCF calculations were tightly converged (TightSCF) with unrestricted spin (UKS). Numerical integrations during all DFT calculations were done on a dense grid (ORCA grid4) while the final run on denser one (ORCA grid5) was also performed.

## Results and Discussion

### DFT calculations

Theoretical calculations on **2** in the gas phase were performed to shed light on the controversial structure of **2**.<sup>17,19,20</sup> Although CASSCF method would be preferable, the computational demand for a structure optimization at this level of theory would be too high and we thus resorted to DFT. The structure was optimized with both symmetric and unsymmetric distributions of chromium(II) ions

as guess geometries, to be sure to start the optimization close to two possible different minima. In spite of the shallow potential energy surface, DFT succeeded in finding two different minima. The unsymmetric structure was found more stable than the symmetric one by about 2.9 kcal mol<sup>-1</sup>. When solvent effects (CH<sub>2</sub>Cl<sub>2</sub>) were included through the COSMO model, the difference in energy between the two minima increased by only 1 kcal mol<sup>-1</sup> in favour of the unsymmetric form with no significant effect on structural parameters of interest, which are reported in Table 1 (for convenience, we number chromium ions as Cr1, Cr2... Cr5 along the chain). In the symmetric structure (Figure 1a) the two inner Cr-Cr distances (Cr2-Cr3 and Cr3-Cr4) are shorter (2.21-2.22 Å) than Cr1-Cr2 and Cr4-Cr5 (2.31-2.32 Å). In the unsymmetric structure (Figure 1b) the C<sub>2</sub> symmetry element located on Cr3 is lost and an alternation of short (1.86-1.90 Å) and long (2.55-2.60 Å) separations results, which matches the experimental interpretation of X-ray data using a “split-atom” model.<sup>19,20</sup> It is worth mentioning that the computed value of about 1.9 Å for the shortest Cr-Cr separation is in agreement with the usual distance associated to a formally fourth-order Cr-Cr bond.<sup>39</sup>

**Table 1.** Cr-Cr distances (Å) in solvatomorphs of **2**, as experimentally found in the solid state at 213 K and as resulting from DFT calculations.

	Cr1-Cr2	Cr2-Cr3	Cr3-Cr4	Cr4-Cr5	Ref.
<b>2</b> ·CH <sub>2</sub> Cl <sub>2</sub>	2.578(7)	1.901(6)	2.587(6)	2.031(6)	<sup>19</sup>
<b>2</b> ·Et <sub>2</sub> O	2.661(3)	1.862(3)	2.644(3)	1.931(3)	<sup>20</sup>
<b>2</b> ·4CHCl <sub>3</sub> ·2Et <sub>2</sub> O	2.598(3)	1.872(2)	2.609(2)	1.963(3)	<sup>20</sup>
DFT – symmetric (gas phase)	2.319	2.207	2.221	2.308	this work
DFT – unsymmetric (gas phase)	2.550	1.862	2.606	1.904	this work
DFT – symmetric (CH <sub>2</sub> Cl <sub>2</sub> )	2.308	2.205	2.220	2.318	this work
DFT – unsymmetric (CH <sub>2</sub> Cl <sub>2</sub> )	2.550	1.852	2.612	1.880	this work

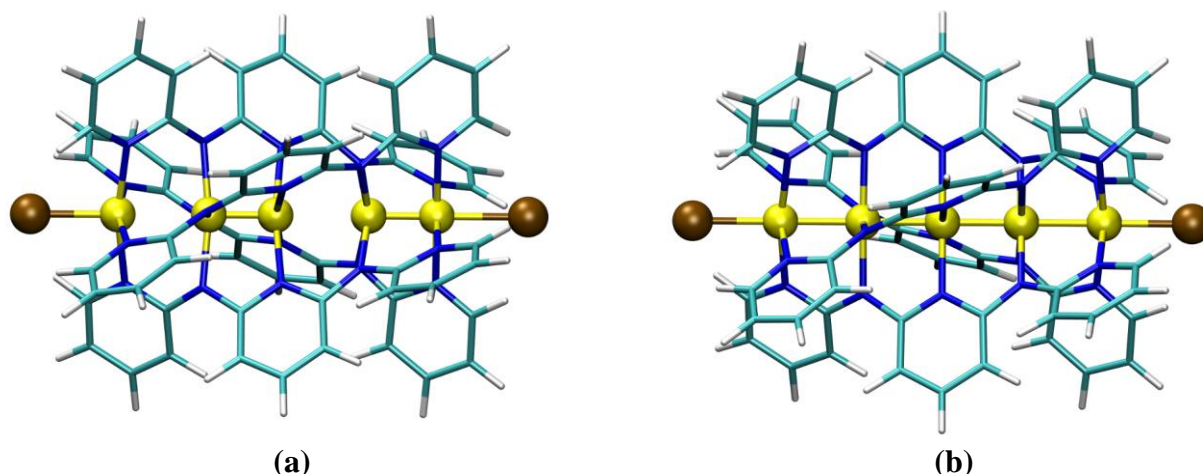
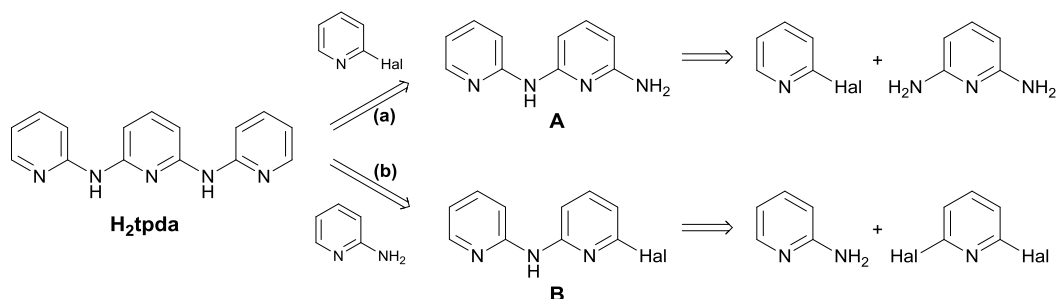


**Figure 1.** Optimized structures of **2**: unsymmetric (a) and symmetric (b). Colour code: yellow = Cr, brown = Cl, blue = N, cyan = C, white = H. Chromium ions are numbered as Cr1, Cr2,...Cr5 from left to right.

**An improved metal-free synthesis of H<sub>2</sub>tpda.** Although the first H<sub>2</sub>tpda-based EMACs were isolated by Peng's group as early as in 1997,<sup>40</sup> an efficient and reliable method to prepare H<sub>2</sub>tpda is still publicly unavailable. In principle, two different synthetic schemes based on nucleophilic aromatic substitution (S<sub>N</sub>Ar) reactions can be identified (Scheme 2): either 2,6-diaminopyridine is reacted with two equivs. of 2-halopyridine *via* intermediate **A** (path a), or 2,6-dihalopyridine is combined with two equivs. of 2-aminopyridine through intermediate **B** (path b).



**Scheme 2.** Retrosynthetic approaches to H<sub>2</sub>tpda.

The two paths differ in one important respect: **B** will hardly proceed to H<sub>2</sub>tpda through an S<sub>N</sub>Ar mechanism, as its electrophilicity is lowered by the electrodonating (aryl)amino substituent. By contrast, the same electronic effect is expected to enhance the nucleophilicity of the primary amino group in **A**, that should promptly react to yield the target compound (these considerations do not apply to Pd-catalyzed reactions, which were in fact predominantly carried out following path (b), *vide infra*). Literature data on the reactivity of 2,6-dibromopyridine with 2,6-diaminopyridine (Figure S1) confirm this view.<sup>41,42</sup> The first-described synthesis of H<sub>2</sub>tpda also followed path (a): starting from 2,6-diaminopyridine, 2-bromopyridine (4.2 equiv.) and an added base (*t*BuOK, 3.0 equiv.) in tetrahydrofuran (THF), the desired product was obtained in modest yield (26%) after

recrystallization.<sup>40</sup> Shortly after, a much higher yield (60%) was claimed by the same group upon replacing 2-bromopyridine with 2.2/2.5 equiv. of 2-chloropyridine and working in refluxing benzene.<sup>43-45</sup> A different group reported comparable yields in crude product by refluxing 2,6-diaminopyridine, 2-bromopyridine (4.0 equiv.) and NaH (3.0 equiv.) in THF.<sup>46</sup> In our hands Peng's method worked at its best using NaH (3.0 equiv.) and a large excess of 2-chloropyridine (14 equiv.), with no solvent. After 3 days at reflux (165°C) under dinitrogen, workup and recrystallization from 2-propanol or methanol afforded pure H<sub>2</sub>tpda in yields that never exceeded 50%. The use of a large excess of 2-chloropyridine, a substance with acute inhalation and dermal toxicity, makes this route even less appealing.

It is known that key factors for an efficient *N*-arylation of 2-aminopyridines with a 2-halopyridine (or a 2-alkoxypyridine) are an appropriate choice of the base and of the solvent.<sup>47,48</sup> Sometimes microwave irradiation is helpful,<sup>49,50</sup> but the most popular way to improve the process is to use a Pd-catalyzed cross coupling method, known as the Buchwald-Hartwig amination.<sup>51,52</sup> Only marginal cases involve a copper-based catalyst, as in the Goldberg reaction.<sup>53</sup> In fact, Pd-catalyzed reactions were extensively used for the synthesis of oligo- $\alpha$ -pyridylamines and related ligands.<sup>10,12,28,54-57</sup> For instance, Buchwald-Hartwig method was followed to prepare an isomer of H<sub>2</sub>tpda, namely *N*<sup>2</sup>,*N*<sup>6</sup>-bis(pyridin-4-yl)pyridine-2,6-diamine (64%),<sup>58</sup> alkyl-substituted congeners of H<sub>2</sub>tpda (51-65%)<sup>57,59</sup> and apparently even H<sub>2</sub>tpda itself (though details were not provided).<sup>60</sup>

Looking for an alternative approach to the Pd-free synthesis of H<sub>2</sub>tpda, we explored the reactivity of 2-fluoropyridine, which is less toxic than 2-chloropyridine and is a known efficient electrophile in S<sub>N</sub>Ar with anilines or other amines.<sup>61-64</sup> The order of addition of the reagents was inspired by the best available method, namely the synthesis of Br<sub>2</sub>H<sub>2</sub>tpda.<sup>42</sup> Thus, the selected base (10 equiv.) was added to solid 2,6-diaminopyridine under Ar and stirred for 10' at r.t.. Then 2-fluoro or 2-chloropyridine (4.0 equiv.) and the solvent (10 mL/mmol of 2,6-diaminopyridine) were sequentially added and the reaction mixture was heated at reflux for 6 h, with final monitoring by TLC. From our survey, we concluded that 2-fluoropyridine converts 2,6-diaminopyridine more efficiently than 2-chloropyridine, while *t*BuOK and alkali-metal hydrides (LiH, NaH) are superior to other bases like Na<sub>2</sub>CO<sub>3</sub>, K<sub>3</sub>PO<sub>4</sub>,<sup>47,48</sup> NaOH, NaOEt or Na<sup>0</sup>. Contrary to our reference literature report,<sup>42</sup> THF did not perform well with respect to toluene, DMSO or DMF, probably due to its lower boiling point. To facilitate reaction workup, toluene was finally chosen as the standard solvent for subsequent work.

In a more focused study on the reaction between 2,6-diaminopyridine, 2-fluoropyridine and LiH in toluene, we discovered that the addition of pyridine (py) as co-solvent causes vigorous hydrogen evolution upon heating. Further experimentation indicated that py is an essential ingredient, as it

promotes the formation of intermediate **A** (Scheme 2) even at r.t., and permits its conversion to H<sub>2</sub>tpda upon heating. However, neither replacing py with more basic 2-ethylpyridine or 2,6-lutidine, nor adding small amounts of 4-(dimethylamino)pyridine improved the results. Final refinements brought the method at its best, being now able to operate over a short reaction time (3 h 15'), with minimal tar formation and using only 3.0 equiv. of 2-fluoropyridine. The crude material is a brownish solid which can be purified by digestion, affording spectroscopically pure H<sub>2</sub>tpda as a beige solid with excellent overall yield (90%). The room temperature <sup>1</sup>H NMR spectrum in DMSO-*d*<sub>6</sub>, presented in Figure 2a, shows seven signals and is thus consistent with C<sub>2v</sub> molecular symmetry in solution; chemical shifts and multiplicities compare well with available literature data<sup>46</sup> (spectral data in Ref. <sup>44</sup> are in part erroneous).

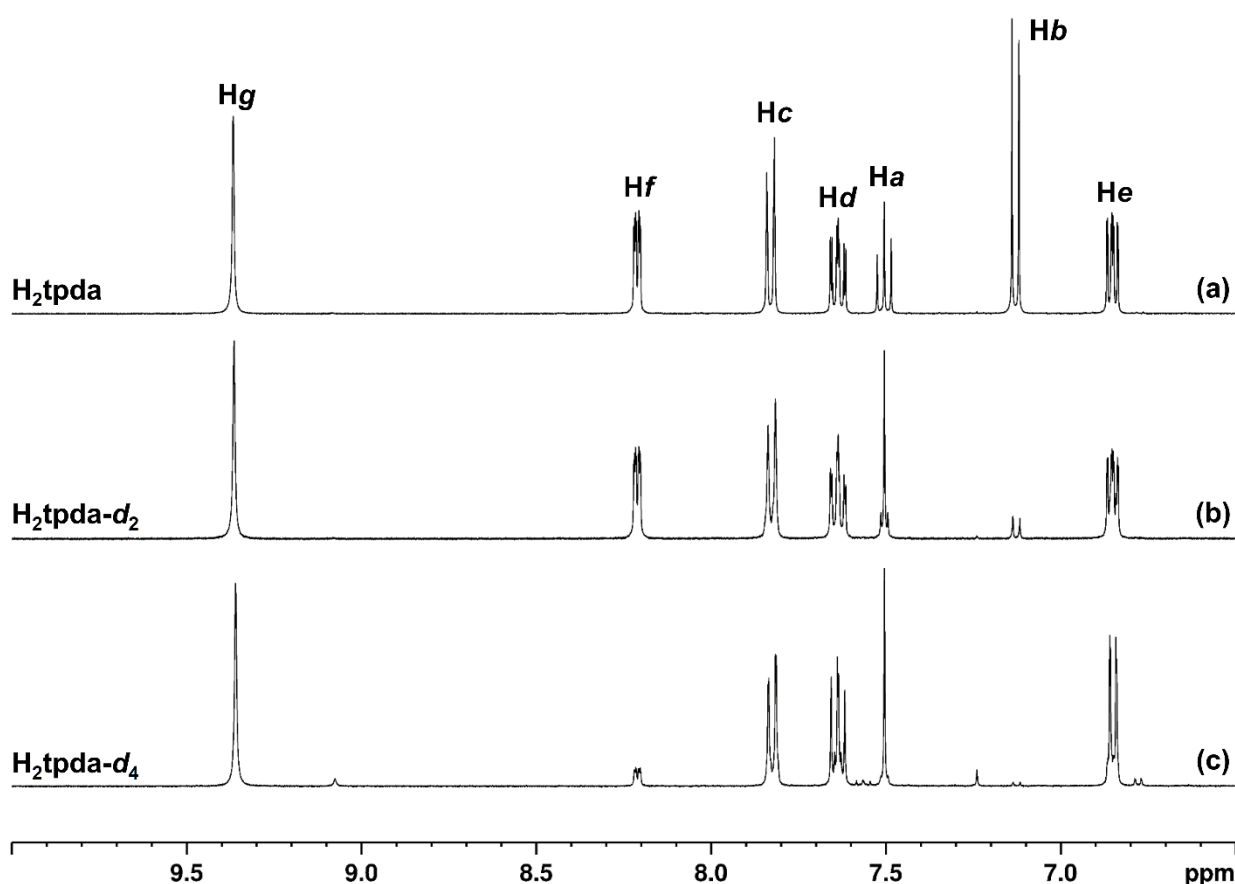
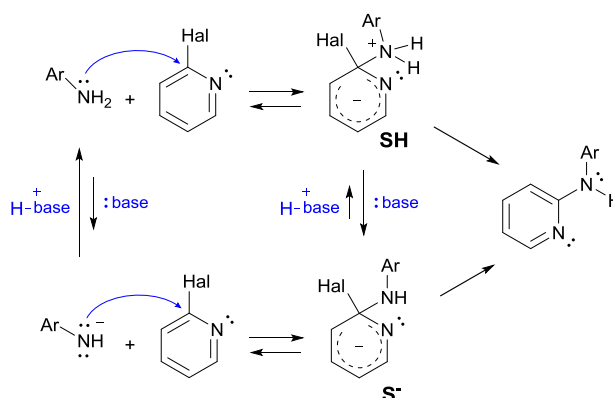


**Figure 2.** Proton NMR spectra of H<sub>2</sub>tpda (a), H<sub>2</sub>tpda-*d*<sub>2</sub> (b) and H<sub>2</sub>tpda-*d*<sub>4</sub> (c). For the labelling scheme, see Scheme 1.

A wealth of theoretical and experimental data support an addition-elimination mechanism for S<sub>N</sub>Ar, with the formation of an intermediate cyclohexadienyl anion with broken benzenoid resonance.<sup>65</sup> Either the formation or the decomposition of this intermediate, also known as a σ-complex (SH or S<sup>-</sup> in Scheme 3) may be rate determining. However, its stability is a major predictor of overall substitution rate, due to the structural and energetic similarity to the involved transition states.<sup>66,67</sup> The interaction of neutral nucleophiles such as amines on deactivated rings

such as halopyridines likely encompasses the formation of a zwitterionic  $\sigma$ -adduct (SH in Scheme 3), consistent with the observation of base catalysis of its decomposition.<sup>68,69</sup>

The nature of the nucleophile greatly influences the features of the  $\sigma$ -complex and the mobility of the halide leaving group, depending on the relative energy of the transition states of formation vs. decomposition of SH. When the formation of SH is rate determining, the halogen nucleofugality order  $F > Cl \approx Br$  is often encountered; conversely, when C-Hal bond is broken in the rate determining step, the opposite reactivity order is found to prevail ( $I > Br > Cl > F$ ).<sup>70</sup> Therefore, the case under study best fits with a rate determining formation of SH.



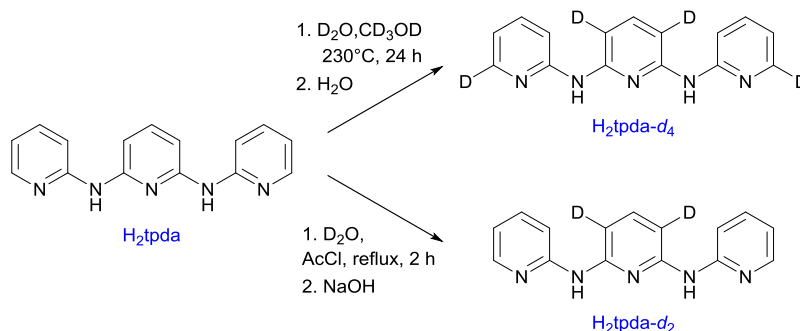
**Scheme 3.**  $S_NAr$  mechanism in the case of neutral and anionic nucleophiles.

In any case, due to the interaction between its components, the system stands on a faint balance, where narrow concentration ranges of the constituents give optimal efficiency. Other factors, including the nature of the added base and the solvent, are also expected to play an important role. A correct choice of the base can be essential, since a too strong base would cause undesired reactions on halopyridines (e.g.  $S_{RN}1$ ).<sup>71</sup> Investigations of  $S_NAr$  involving amine nucleophiles in aprotic solvents have revealed a complex base catalysis behaviour that could be rationalized by supposing the initial formation of a molecular charge-transfer complex between the nucleophile and the electrophilic aromatic ring.<sup>72-74</sup> The choice of the solvent holds a similar importance.<sup>75</sup> Polar aprotic solvents should result in increased stabilization of SH, while protic (hydrogen donor) solvents often adversely affect the overall rate, possibly due to excessive solvation of the nucleophile. Nevertheless, the crucial role played by pyridine in the case under study is at present unexplained.

### Post-synthetic isotopic labelling of H<sub>2</sub>tpda

Although deuterio-debromination of Br<sub>2</sub>H<sub>2</sub>tpda<sup>76</sup> might provide a route to the selective deuteration of H<sub>2</sub>tpda on *f* positions, we preferred to test post-synthetic labelling. H/D exchange was then monitored following prolonged heating at 220-230°C in a 400-fold excess of D<sub>2</sub>O inside a pressure

resistant stainless steel vessel with a screw cap.<sup>77</sup> The product was obtained as a beige solid in good yield by washing the raw reaction mixture with water to remove some decomposition product visible in TLC (this treatment causes partial back exchange of N-D groups to N-H; deuteration of amino groups can be restored by boiling in CD<sub>3</sub>OD and evaporating the solvent). The first trials showed that both H<sub>b</sub> and H<sub>f</sub> (Scheme 1) hydrogens undergo exchange (Scheme 4), as evident from the reduced intensity of the corresponding <sup>1</sup>H NMR peaks at 7.13 and 8.21 ppm (see Figure 2c; scale-expanded spectra are available in Figure S2).



**Scheme 4.** Isotopic labelling of H<sub>2</sub>tpda.

We also found that internal positions *b* exchange faster than *f* positions. Considering that the acid H/D exchange should follow a S<sub>E</sub>Ar mechanism, the high conjugation between the central pyridine ring and two arylamino substituents is likely to play a role.<sup>78</sup> However, using pure D<sub>2</sub>O as a reaction medium gave poorly reproducibility, presumably due to the low solubility of H<sub>2</sub>tpda in water. Addition of 5-6% (v/v) of CD<sub>3</sub>OD as a co-solvent was beneficial and afforded 96-98 D% at *b* and 63-83 D% at *f* positions (H<sub>2</sub>tpda-*d*<sub>4</sub>). Beyond directly affecting the intensity of H<sub>b</sub> and H<sub>f</sub> signals, deuteration results in a clear modification of the hyperfine coupling patterns for neighboring protons (Figures 2c and S2). The hyperfine pattern for protons H<sub>c</sub> at 7.83 ppm, for instance, changes from a doublet-of-pseudo-triplets (<sup>3</sup>*J*(*c*,*d*) >> <sup>4</sup>*J*(*c*,*e*) ~ <sup>5</sup>*J*(*c*,*f*)) to a doublet-of-doublets upon deuteration of *f* positions. Similarly, the ddd pattern of protons H<sub>e</sub> at 6.85 ppm (<sup>3</sup>*J*(*e*,*d*) > <sup>3</sup>*J*(*e*,*f*) > <sup>4</sup>*J*(*e*,*c*)) turns into a simpler dd. Finally, the triplet of protons H<sub>a</sub> in nondeuterated H<sub>2</sub>tpda (7.50 ppm) becomes a singlet upon deuteration of *b* positions. The H<sub>c</sub> integrated intensity ranged from 1.99 to 1.91H, signalling that isotopic enrichment up to a few percent can also occur at these positions.

Deuteron NMR spectroscopy provided complementary information on H/D exchange. The H<sub>2</sub>tpda-*d*<sub>4</sub> sample that afforded the spectrum in Figure 2c, dissolved in nondeuterated DMSO, gave two main <sup>2</sup>H resonances at 8.2 and 7.1 ppm, with FWHM of 20-25 Hz (Figure 3). By direct comparison with the chemical shift values in proton spectra, the two peaks are assigned to D<sub>f</sub> and



*Db* nuclei, while the shoulder at 7.8 ppm confirms that *Hc* protons also undergo minor H/D exchange. Finally, the weak broad peak at 9.3 ppm is attributed to residual N-D groups.

Occasionally, using a 200-fold molar excess of D<sub>2</sub>O we reached 90.5 and 15.5 D% on the two positions, respectively (H<sub>2</sub>tpda-*d*<sub>2</sub>, see Figures 2b and S2). A similar selective exchange of *b* positions was later shown to occur by simply refluxing H<sub>2</sub>tpda with a solution of DCl in CH<sub>3</sub>COOD/D<sub>2</sub>O 1:5 (v/v) for 2 h (Figures S3 and S4).

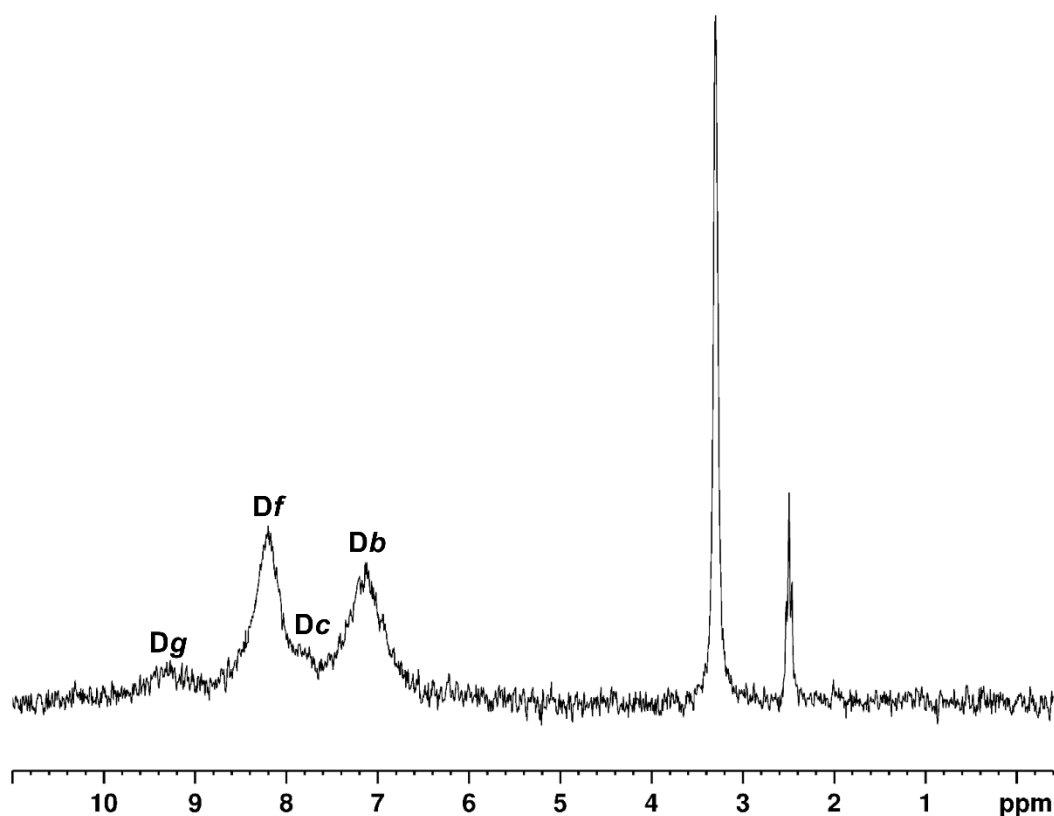


**Figure 3.** Deuteron NMR spectra of H<sub>2</sub>tpda-*d*<sub>4</sub> in DMSO. The sharp peaks at 2.50 and 3.30 ppm arise from deuterium naturally present in DMSO and water.

**Solution properties of [Cr<sub>5</sub>(tpda)<sub>4</sub>Cl<sub>2</sub>] (**2**), [Cr<sub>5</sub>(tpda-*d*<sub>2</sub>)<sub>4</sub>Cl<sub>2</sub>] (**2-d**<sub>8</sub>) and [Cr<sub>5</sub>(tpda-*d*<sub>4</sub>)<sub>4</sub>Cl<sub>2</sub>] (**2-d**<sub>16</sub>).**

Crystalline samples of pentachromium(II) strings **2**, **2-d**<sub>8</sub> and **2-d**<sub>16</sub> were prepared as tetrakis(chloroform) bis(diethylether) solvates following literature procedures.<sup>15,17</sup> Synthetic conditions require refluxing the reaction mixture in boiling naphthalene for several hours and might lower the isotopic enrichment of the ligand. Therefore, the crystalline material so obtained was preliminarily characterized by ESI-MS in CH<sub>2</sub>Cl<sub>2</sub>. Scale expanded spectra are compared in Figure 4 (full scale spectra are available in Figure S5). The molecular ion peaks are detected at *m/z* = 1376.2, 1383.1 and 1389.2, respectively, confirming increasing isotopic enrichment across the series. The isotopic patterns were analyzed by assuming that only *Hb* hydrogens are susceptible of H/D back

exchange. The H/D ratios at the remaining positions were thus held fixed at the values determined by proton NMR (see Experimental Section). The best agreement with experimental patterns is achieved with 70 and 96 D% at *b* positions in **2**-*d*<sub>8</sub> and **2**-*d*<sub>16</sub>, respectively, indicating good to excellent persistence of D content.

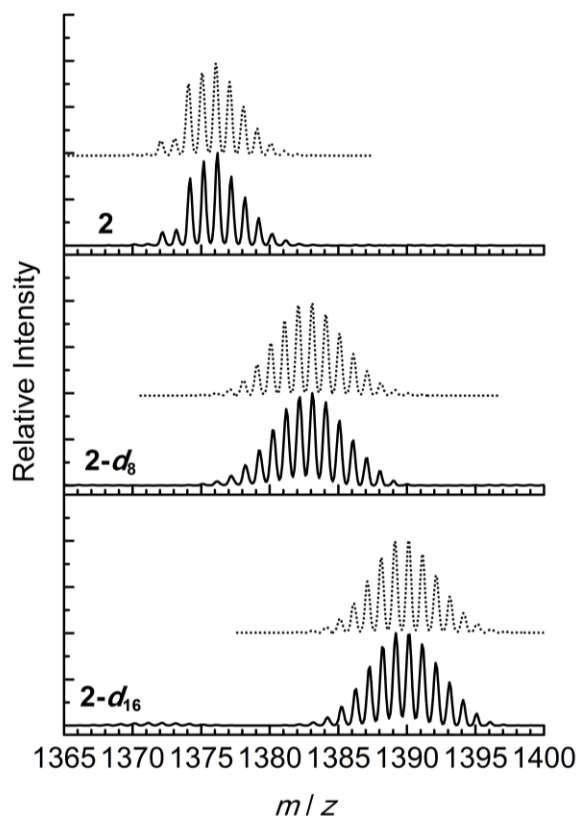


**Figure 4.** Scale expanded ESI-MS spectra of **2**, **2**-*d*<sub>8</sub> and **2**-*d*<sub>16</sub> (direct infusion, CH<sub>2</sub>Cl<sub>2</sub>, positive ion mode). Each graph shows the comparison between the experimental (solid line) and simulated (dotted line) isotopic patterns of molecular ion peaks at  $m/z = 1376.2$ ,  $1383.1$  and  $1389.2$  (from top to bottom).

Solutions of **2** in dichloromethane are indefinitely stable at room temperature in the absence of dioxygen. The <sup>1</sup>H NMR spectrum of a solution of **2** in CD<sub>2</sub>Cl<sub>2</sub> is shown in Figure 5a. Beside narrow peaks arising from solvent residuals and other impurities, the spectrum is dominated by five very broad (10<sup>2</sup>-10<sup>3</sup> Hz) and paramagnetically-shifted resonances of ligand protons at 13.0, 2.3, 1.0, 0.1 and -10.2 ppm. No other peaks are visible in a spectral window ranging from -80 to 80 ppm.

As shown in Scheme 1 and Figure 2a, H<sub>2</sub>tpda ligand in solution contains six magnetically inequivalent C-H protons<sup>79</sup> (vs. four in Hdpa). Assuming that the complex has at least fourfold symmetry in solution, *i.e.* that the four tpda<sup>2-</sup> ligands are equivalent, the expected number of resonances is *six* for a symmetric (over NMR timescale) *D*<sub>4</sub> structure and *eleven* for an unsymmetric *C*<sub>4</sub> one. This is exactly the number of NMR resonances detected for [Ni<sub>5</sub>(tpda)<sub>4</sub>(SCN)<sub>2</sub>] and [NiRu<sub>2</sub>Ni<sub>2</sub>(tpda)<sub>4</sub>(SCN)<sub>2</sub>], which have a symmetric and an unsymmetric framework, respectively.<sup>79</sup>

An unsymmetric structure would also entail a highly nonuniform spin density along the chain, with a localized high-spin ( $S = 2$ ) chromium(II) center at one extreme flanked by two quadruply-bonded  $\text{Cr}_2^{4+}$  pairs towards the other extreme. The dichromium(II) paddlewheel complex  $[\text{Cr}_2(\text{dpa})_4]$  contains one such pair and is a virtually diamagnetic molecule. By consequence, its proton NMR signals are detected in the usual range for aromatic C-H groups and give resolvable hyperfine splittings.<sup>80</sup> The number, width, and chemical shift of the observed proton NMR resonances coherently suggest that **2** is symmetric over NMR timescale and that one resonance out of six is paramagnetically broadened beyond detection. This missing resonance is presumably that from *ortho*-pyridyl protons H*f*, which lie closest to the paramagnetic centers. This interpretation is confirmed by the  $^1\text{H}$  NMR spectra of **2**-*d*<sub>8</sub> and **2**-*d*<sub>16</sub> (Figure 5b,c). The two spectra feature the same ligand peaks as in Figure 5a, except for the signal around 1.0 ppm, which is strongly reduced in intensity. The observation that deuteration of *f* positions has no impact on proton spectra proves that *ortho*-pyridyl protons are undetectable.  $^2\text{H}$  NMR spectroscopy on the same samples of Figures 5b,c lends even more direct support to the proposed scenario. For both isotopic enrichments, a single paramagnetically-shifted resonance is detected at 0.8-0.9 ppm (Figure 6), hence close to the position of the  $^1\text{H}$  peak that disappears upon deuteration of *b* positions. Notice that such a resonance has a FWHM of ca. 40 Hz and is thus significantly sharper than found in proton spectra, a known advantage of  $^1\text{H}$  over  $^2\text{H}$  NMR spectroscopy for the investigation of paramagnetic systems.<sup>81</sup> The observation of a single peak of *D**b* nuclei is also consistent with a symmetric ( $D_4$ ) structure over NMR timescale. In fact, for an unsymmetric ( $C_4$ ) structure featuring an alternation of long and short Cr...Cr separations (as in the solid state) the two *D**b* nuclei of each ligand would be inequivalent and would give two distinct signals. One possibility is that the structure is truly symmetric in solution (Scheme 1a). This option is however ruled out by our DFT studies, which indicate that the ground state of **2** entails an alternation of long and short Cr-Cr distances. We contend that fast oscillation between the two equivalent unsymmetrical structures (Scheme 1b,c) affords average  $D_4$  symmetry and explains all our experimental results. Taking the energy difference between symmetric and unsymmetric forms (3.9 kcal/mol in  $\text{CH}_2\text{Cl}_2$ ) as the activation energy for the interconversion, the oscillation rate at room temperature is expected to be much faster than the chemical shift difference between the observed NMR signals (ca. 10-20 ppm, i.e. 4000-8000 Hz at 400 MHz). The fast exchange regime is thus attained and the oscillation is averaged out over NMR timescale.<sup>82</sup>

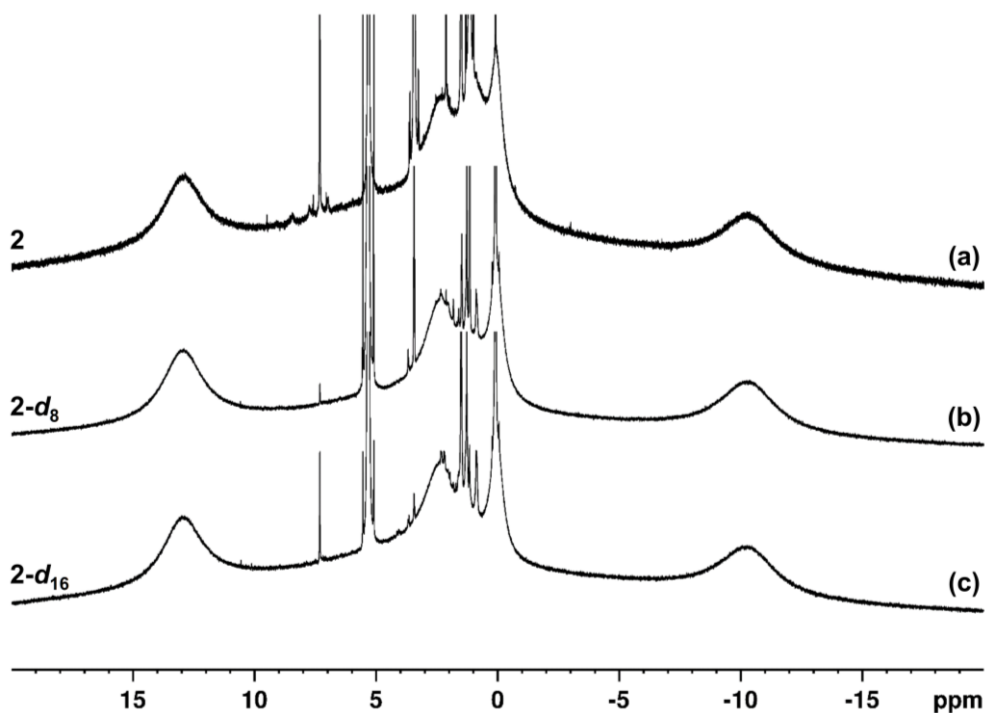


**Figure 5.**  $^1\text{H}$  NMR spectra of **2** (a),  $2\text{-}d_8$  (b) and  $2\text{-}d_{16}$  (c) in  $\text{CD}_2\text{Cl}_2$ .

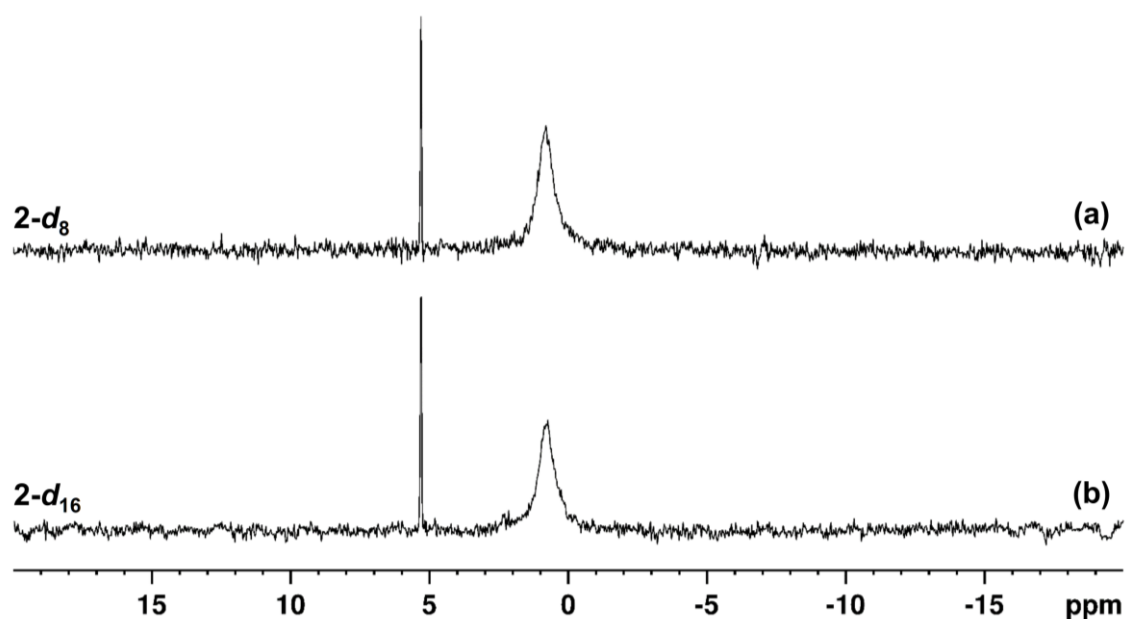


**Figure 6.** Deuteron NMR spectra of  $2\text{-}d_8$  (a) and  $2\text{-}d_{16}$  (b) in  $\text{CH}_2\text{Cl}_2$ . The sharp peak at 5.32 ppm arises from deuterium naturally present in  $\text{CH}_2\text{Cl}_2$ .

## Conclusions

With our study, we have demonstrated the applicability of isotopic (D) labelling and solution  $^1\text{H}/^2\text{H}$  NMR spectroscopies to probe the structure of paramagnetic EMACs of relevance in molecular electronics and magnetism, such as  $[\text{Cr}_5(\text{tpda})_4\text{Cl}_2]$  (**2**). A reliable, Pd-free synthetic route has been developed to prepare  $\text{H}_2\text{tpda}$  from 2,6-diaminopyridine and 2-fluoropyridine, with yield (90%)

largely surpassing that of the best published methods.<sup>43-46</sup> H/D exchange procedures have then been devised to allow deuteration at *b* positions only (H<sub>2</sub>tpda-*d*<sub>2</sub>), or at both *b* and *f* positions (H<sub>2</sub>tpda-*d*<sub>4</sub>, see Scheme 1). The complementary information provided by <sup>1</sup>H and <sup>2</sup>H NMR spectra of **2**, **2**-*d*<sub>8</sub> and **2**-*d*<sub>16</sub> in dichloromethane demonstrates that *ortho*-pyridyl hydrogens are undetectable in these complexes, presumably due to their close proximity to the paramagnetic centers. The five paramagnetically-broadened and shifted signals observed in proton spectra, *plus* this invisible resonance, exactly match the number of inequivalent hydrogens expected for a symmetric (*D*<sub>4</sub>) structure.

Similar spectroscopic features have been reported for trichromium(II) complex [Cr<sub>3</sub>(dpa)<sub>4</sub>(N<sub>3</sub>)<sub>2</sub>] (**3**).<sup>26</sup> From room-temperature to –50°C only *three* resonances of dpa<sup>–</sup> protons are observed in the <sup>1</sup>H-NMR spectrum of **3**·Et<sub>2</sub>O in CD<sub>2</sub>Cl<sub>2</sub> solution.<sup>26</sup> In these complexes of dpa<sup>–</sup>, a symmetric (*D*<sub>4</sub>) structure would afford *four* inequivalent protons, while an unsymmetric (*C*<sub>4</sub>) structure would contain *eight* inequivalent protons. The authors argued that a symmetric structure is most probably adopted over the timescale of NMR experiment, with one signal paramagnetically shifted and broadened beyond detection (based on our results, the signal from *ortho*-pyridyl protons). DFT calculations have shown that in trichromium(II) EMACs (except those containing very weak axial ligands) the asymmetric stretching of the Cr<sub>3</sub> unit is a very soft mode and that the potential energy surface features a single minimum corresponding to the *symmetric* structure.<sup>23,24</sup> The symmetry emerging from NMR spectra thus reflects the actual ground symmetry of **3**, although a large asymmetric stretching amplitude is expected.

At difference with this, DFT studies on **2** in the gas phase and including CH<sub>2</sub>Cl<sub>2</sub> solvent effects indicate that the two equivalent unsymmetric forms are more stable (by 2.9 and 3.9 kcal/mol, respectively) than the symmetric one; by consequence, the high symmetry displayed by **2** in CH<sub>2</sub>Cl<sub>2</sub> is likely explained by a hopping processes occurring at a rate faster than NMR timescale. In spite of their different energy landscapes, then, strings **2** and **3** both display their maximum possible symmetry (*D*<sub>4</sub>) on the timescale of NMR experiment.

It remains to be elicited if the symmetric and unsymmetric forms of **2** may be stable as separate, slowly switching entities, as postulated to explain the bimodal single-molecule conductance of [Cr<sub>5</sub>(tpda)<sub>4</sub>(SCN)<sub>2</sub>].<sup>4</sup> In STM break-junction experiments,<sup>4b</sup> two sets of conductance values were found, namely 48.8(1.0)·10<sup>–4</sup> and 9.5(1.2)·10<sup>–4</sup> G<sub>0</sub> (G<sub>0</sub> is the conductance quantum), which were assigned to the symmetric (delocalized, more conducting) and unsymmetric (localized, less conducting) forms, respectively. The heptachromium(II) congener also exhibits two conductance values.<sup>4a</sup> However, low-symmetry distortions do not necessarily have such a large impact on electron transport, and DFT calculations on trichromium(II) EMACs have indeed predicted an

opposite trend.<sup>2,3c</sup> More important, precise structural information on the existence of pentachromium(II) strings in symmetric form is still lacking. Based on surface-enhanced Raman spectra, the two isomers were claimed to coexist when molecules are bound to metal nanoparticles in solution, but solid experimental evidence is still lacking.<sup>29</sup> In fact, contrary to the assertion made in Ref.,<sup>29</sup> the X-ray data in Refs. <sup>17</sup> (Peng's group) and <sup>21</sup> (Cotton's group) do not show the existence of both symmetric and unsymmetric forms; rather, these and other papers<sup>19,20</sup> discuss two distinct structural models which differ in the *neglection*<sup>17</sup> or *inclusion*<sup>19-21</sup> of positional disorder effects. That positional disorder may be present is suggested by the otherwise distinctly prolate displacement ellipsoids of the Cr ions along the chain axis and by the lower *wR2* index achieved using a "split atom" model.<sup>21</sup> We cannot at present exclude that, under special circumstances not captured by our DFT calculations, a symmetric complex may become stable in the solid state. However, since our DFT studies indicate that in the gas phase and in solution the symmetric form has a distinctly higher energy than the unsymmetric one, the existence of a stable symmetric complex without the rigid constraints of a crystal lattice would be, in our view, quite surprising.

## Acknowledgements

A. D. gratefully acknowledges the University of Warwick (UK) for an Erasmus+ Placement fellowship during his work in Modena (Italy). We thank A. Mucci (Department of Chemical and Geological Sciences) for stimulating discussion on dynamic NMR spectroscopy.

## References

- 1 Y. Tanaka, M. Kiguchi and M. Akita, *Chem. Eur. J.* 2017, **23**, 4741–4749.
- 2 V. P. Georgiev, P. J. Mohan, D. DeBrincat and J. E. McGrady, *Coord. Chem. Rev.*, 2013, **257**, 290–298.
- 3 (a) P. J. Mohan, V. P. Georgiev and J. E. McGrady, *Chem. Sci.*, 2012, **3**, 1319–1329; (b) V. P. Georgiev, W. M. C. Sameera and J. E. McGrady, *J. Phys. Chem. C*, 2012, **116**, 20163–20172; (c) V. P. Georgiev and J. E. McGrady, *J. Am. Chem. Soc.*, 2011, **133**, 12590–12599.
- 4 (a) I.-W. P. Chen, M.-D. Fu, W.-H. Tseng, J.-Y. Yu, S.-H. Wu, C.-J. Ku, C. Chen and S.-M. Peng, *Angew. Chem., Int. Ed.*, 2006, **45**, 5814–5818; (b) T.-C. Ting, L.-Y. Hsu, M.-J. Huang, E.-C. Horng, H.-C. Lu, C.-H. Hsu, C.-H. Jiang, B.-Y. Jin, S.-M. Peng and C.-h. Chen, *Angew. Chem., Int. Ed.*, 2015, **54**, 15734–15738.
- 5 (a) K. Uemura, *Dalton Trans.*, 2017, **46**, 5474–5492; (b) G. Aromi, *Comments Inorg. Chem.*, 2011, **32**, 163–194.

- 6 J. F. Berry, F. A. Cotton, L. M. Daniels, C. A. Murillo and X. Wang, *Inorg. Chem.*, 2003, **42**, 2418–2427.
- 7 J. F. Berry, *Struct. Bond.*, 2010, **136**, 1–28.
- 8 (a) S.-A. Hua, M.-C. Cheng, C. Chen and S.-M. Peng, *Eur. J. Inorg. Chem.*, 2015, 2510–2523; (b) S.-A. Hua, Y.-C. Tsai and S.-M. Peng, *J. Chin. Chem. Soc.* 2014, **61**, 9–26.
- 9 I. Po-Chun Liu, W.-Z. Wang and S.-M. Peng, *Chem. Commun.*, 2009, 4323–4331.
- 10 H. Hasanov, U.-K. Tan, R.-R. Wang, G. H. Lee and S.-M. Peng, *Tetrahedron Lett.*, 2004, **45**, 7765–7769.
- 11 R. H. Ismayilov, W.-Z. Wang, G.-H. Lee, C.-Y. Yeh, S.-A. Hua, Y. Song, M.-M. Rohmer, M. Bénard and S.-M. Peng, *Angew. Chem., Int. Ed.*, 2011, **50**, 2045–2048.
- 12 P.-J. Chen, M. Sigrist, E.-C. Horng, G.-M. Lin, G.-H. Lee, C. Chen and S.-M. Peng, *Chem. Commun.*, 2017, **53**, 4673–4676.
- 13 D. W. Brogden and J. F. Berry, *Comments Inorg. Chem.*, 2016, **36**, 17–37.
- 14 J. H. Christian, D. W. Brogden, J. K. Bindra, J. S. Kinyon, J. van Tol, J. Wang, J. F. Berry and N. S. Dalal, *Inorg. Chem.*, 2016, **55**, 6376–6383.
- 15 A. Cornia, L. Rigamonti, S. Boccedi, R. Clérac, M. Rouzières and L. Sorace, *Chem. Commun.*, 2014, **50**, 15191–15194.
- 16 R. Clérac, F. A. Cotton, L. M. Daniels, K. R. Dunbar, C. A. Murillo and I. Pascual, *Inorg. Chem.*, 2000, **39**, 748–751.
- 17 H. Chang, J. Li, C. Wang, T. Lin, H. Lee, G. Lee and S. Peng, *Eur. J. Inorg. Chem.*, 1999, 1243–1251.
- 18 J. F. Berry, F. A. Cotton, T. Lu, C. A. Murillo, B. K. Roberts and X. Wang, *J. Am. Chem. Soc.*, 2004, **126**, 7082–7096.
- 19 F. A. Cotton, L. M. Daniels, T. Lu, A. Murillo and X. Wang, *J. Chem. Soc., Dalton Trans.*, 1999, **5**, 517–518.
- 20 F. A. Cotton, L. M. Daniels, C. A. Murillo and X. Wang, *Chem. Commun.*, 1999, **5**, 2461–2462.
- 21 J. F. Berry, F. A. Cotton, C. S. Fewox, T. Lu, C. a Murillo and X. Wang, *Dalton Trans.*,

2004, 2297–2302.

- 22 L.-C. Wu, M. K. Thomsen, S. R. Madsen, M. Schmoekel, M. R. V. Jørgensen, M.-C. Cheng, S.-M. Peng, Y.-S. Chen, J. Overgaard and B. B. Iversen, *Inorg. Chem.*, 2014, **53**, 12489–12498.
- 23 N. Benbellat, M.-M. Rohmer and M. Bénard, *Chem. Commun.*, 2001, **3**, 2368–2369.
- 24 M. Spivak, V. Arcisauskaite, X. López, J. E. McGrady and C. de Graaf, *Dalton Trans.*, 2017, **46**, 6202–6211.
- 25 R. H. Ismayilov, W.-Z. Wang, G.-H. Lee, R.-R. Wang, I. P.-C. Liu, C.-Y. Yeh and S.-M. Peng, *Dalton Trans.*, 2007, **2**, 2898–2907.
- 26 Y. Turov and J. F. Berry, *Dalton Trans.*, 2012, **41**, 8153–8161.
- 27 R. H. Ismayilov, W.-Z. Wang, G.-H. Lee, C.-H. Chien, C.-H. Jiang, C.-L. Chiu, C.-Y. Yeh and S.-M. Peng, *Eur. J. Inorg. Chem.*, 2009, 2110–2120.
- 28 R. H. Ismayilov, W.-Z. Wang, R.-R. Wang, C.-Y. Yeh, G.-H. Lee and S.-M. Peng, *Chem. Commun.*, 2007, 1121–1123.
- 29 Y.-M. Huang, H.-R. Tsai, S.-H. Lai, S. J. Lee, I.-C. Chen, C. L. Huang, S.-M. Peng and W.-Z. Wang, *J. Phys. Chem. C*, 2011, **115**, 13919–13926.
- 30 C.-J. Hsiao, S.-H. Lai, I.-C. Chen, W.-Z. Wang and S.-M. Peng, *J. Phys. Chem. A*, 2008, **112**, 13528–13534.
- 31 G. R. Fulmer, A. J. M. Miller, N. H. Sherden, H. E. Gottlieb, A. Nudelman, B. M. Stoltz, J. E. Bercaw and K. I. Goldberg, *Organometallics*, 2010, **29**, 2176–2179.
- 32 J. E. Redman, *Isotope Distribution Calculator*, Cardiff University, Cardiff, UK, 2005, <http://www.kombyonyx.com/isotopes/> (accessed October 2017).
- 33 F. Neese, The ORCA program system, *Wiley Interdiscip. Rev.: Comput. Mol. Sci.*, 2012, **2**, 73–78.
- 34 J. P. Perdew, K. Burke and M. Ernzerhof, *Phys. Rev. Lett.*, 1996, **77**, 3865–3868.
- 35 S. Grimme, J. Antony, S. Ehrlich and H. Krieg, *J. Chem. Phys.*, 2010, **132**, 154104.
- 36 D. A. Pantazis, X.-Y. Chen, C. R. Landis and F. Neese, *J. Chem. Theory Comput.*, 2008, **4**, 908–919.



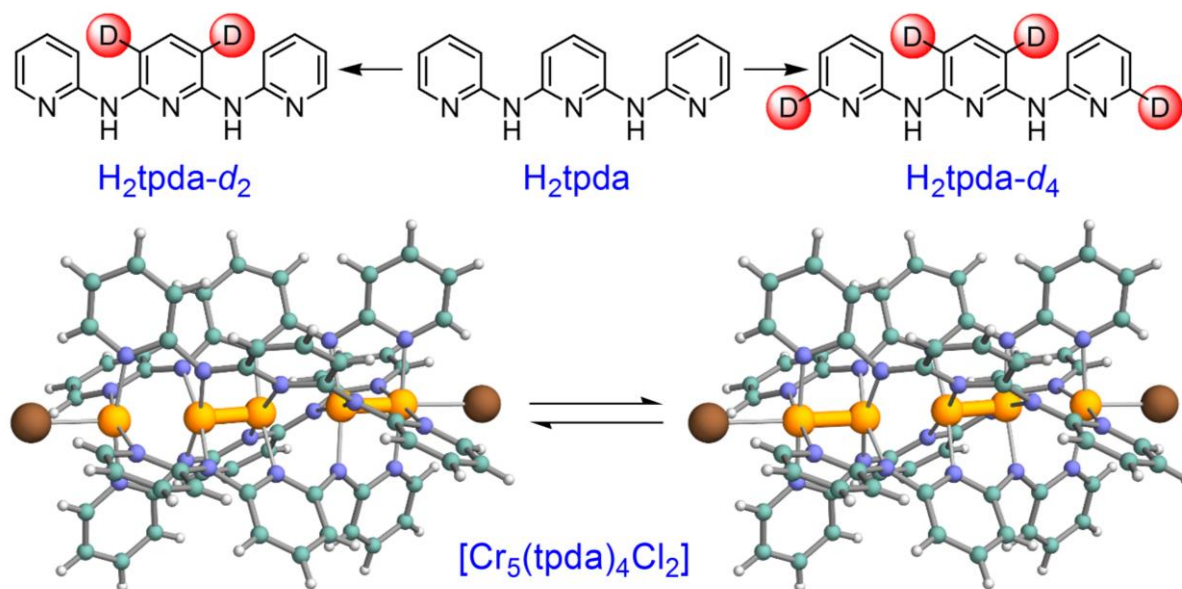
- 37 F. Weigend and R. Ahlrichs, *Phys. Chem. Chem. Phys.*, 2005, **7**, 3297–3305.
- 38 A. Klamt and G. Schüürmann, *J. Chem. Soc., Perkin Trans. 2*, 1993, 799–805.
- 39 M. Brynda, L. Gagliardi and B. O. Roos, *Chem. Phys. Lett.*, 2009, **471**, 1–10.
- 40 S.-J. Shieh, C.-C. Chou, G.-H. Lee, C.-C. Wang and S.-M. Peng, *Angew. Chem., Int. Ed. Engl.*, 1997, **36**, 56–59.
- 41 H. Hasan, U.-K. Tan, Y.-S. Lin, C.-C. Lee, G.-H. Lee, T.-W. Lin and S.-M. Peng, *Inorg. Chim. Acta*, 2003, **351**, 369–378.
- 42 H.-Y. Gong, X.-H. Zhang, D.-X. Wang, H.-W. Ma, Q.-Y. Zheng and M.-X. Wang, *Chem. - Eur. J.*, 2006, **12**, 9262–9275.
- 43 M. Yang, C.-C. Chou, H.-C. Lee, G.-H. Lee, M. Leung and S.-M. Peng, *Chem. Commun.*, 1997, 2279–2280.
- 44 C. Wang, W. Lo, C. Chou, G. Lee, J. Chen and S. Peng, *Inorg. Chem.*, 1998, **37**, 4059–4065.
- 45 C.-Y. Yeh, C.-H. Chou, K.-C. Pan, C.-C. Wang, G.-H. Lee, Y. O. Su and S.-M. Peng, *J. Chem. Soc. Dalton Trans.*, 2002, **5**, 2670–2677.
- 46 K. Ho, W. Yu, K. Cheung and C. Che, *J. Chem. Soc., Dalton Trans.*, 1999, **14**, 1581–1586.
- 47 J. L. Bolliger and C. M. Frech, *Tetrahedron*, 2009, **65**, 1180–1187.
- 48 J. L. Bolliger, M. Oberholzer and C. M. Frech, *Adv. Synth. Catal.*, 2011, **353**, 945–954.
- 49 S. Narayan, T. Seelhammer and R. E. Gawley, *Tetrahedron Lett.*, 2004, **45**, 757–759.
- 50 Y.-J. Cherng, *Tetrahedron*, 2002, **58**, 887–890.
- 51 J. F. Hartwig, in *Handbook of Organopalladium Chemistry for Organic Synthesis*, ed. E.-I. Negishi and A. de Meijere, John Wiley & Sons, New York, Vol. 1., 2002, pp. 1051–1096.
- 52 R. J. Lundgren, A. Sappong-Kumankumah and M. Stradiotto, *Chem. - Eur. J.*, 2010, **16**, 1983–1991.
- 53 K. Kunz, U. Scholz and D. Ganzer, *Synlett*, 2003, 2428–2439.
- 54 M. Leung, A. B. Mandal, C.-C. Wang, G.-H. Lee, S.-M. Peng, H.-L. Cheng, G.-R. Her, I. Chao, H.-F. Lu, Y.-C. Sun, M.-Y. Shiao and P.-T. Chou, *J. Am. Chem. Soc.*, 2002, **124**, 4287–4297.

- 55 R. H. Ismayilov, W.-Z. Wang, G.-H. Lee and S.-M. Peng, *Dalton Trans.*, 2006, 478–491.
- 56 S.-A. Hua, I. P.-C. Liu, H. Hasanov, G.-C. Huang, R. H. Ismayilov, C.-L. Chiu, C.-Y. Yeh, G.-H. Lee and S.-M. Peng, *Dalton Trans.*, 2010, **39**, 3890–3896.
- 57 J. F. Berry, F. A. Cotton, P. Lei, T. Lu and C. A. Murillo, *Inorg. Chem.*, 2003, **42**, 3534–3539.
- 58 C.-J. Wang, H.-R. Ma, Y.-Y. Wang, P. Liu, L.-J. Zhou, Q.-Z. Shi and S.-M. Peng, *Cryst. Growth Des.*, 2007, **7**, 1811–1817.
- 59 C.-X. Yin, J. Su, F.-J. Huo, R.-H. Ismayilov, W.-Z. Wang, G.-H. Lee, C.-Y. Yeh and S.-M. Peng, *J. Coord. Chem.*, 2009, **62**, 2974–2982.
- 60 W.-C. Hung, M. Sigrist, S.-A. Hua, L.-C. Wu, T.-J. Liu, B.-Y. Jin, G.-H. Lee and S.-M. Peng, *Chem. Commun.*, 2016, **52**, 12380–12382.
- 61 P. Stanetty, J. Röhring, M. Schnürch and M. D. Mihovilovic, *Tetrahedron*, 2006, **62**, 2380–2387.
- 62 D. Blomberg, K. Brickmann and J. Kihlberg, *Tetrahedron*, 2006, **62**, 10937–10944.
- 63 M. Castillo, P. Forns, M. Erra, M. Mir, M. López, M. Maldonado, A. Orellana, C. Carreño, I. Ramis, M. Miralpeix and B. Vidal, *Bioorg. Med. Chem. Lett.*, 2012, **22**, 5419–5423.
- 64 K. Seki, K. Ohkura, M. Terashima and Y. Kanaoka, *Heterocycles*, 1994, **37**, 993–996.
- 65 Z. Wu and R. Glaser, *J. Am. Chem. Soc.*, 2004, **126**, 10632–10639.
- 66 S. M. Chiacchiera, J. O. Singh, J. D. Anunziata and J. J. Silber, *J. Chem. Soc., Perkin Trans. 2*, 1987, 987–993.
- 67 J. Miller, *Aromatic Nucleophilic Substitution*, Elsevier, Amsterdam, 1968.
- 68 M. R. Crampton, T. A. Emokpae, J. A. K. Howard, C. Isanbor and R. Mondal, *Org. Biomol. Chem.*, 2003, **1**, 1004–1011.
- 69 M. R. Crampton, T. A. Emokpae, C. Isanbor, A. S. Batsanov, J. A. K. Howard and R. Mondal, *Eur. J. Org. Chem.*, 2006, 1222–1230.
- 70 F. Terrier, in *Modern Nucleophilic Aromatic Substitution*, Wiley-VCH, Weinheim, 2013, ch. 1.

- 71 M. B. Smith, *March's Advanced Organic Chemistry: Reactions, Mechanisms, and Structure*, John Wiley & Sons, New York, 7th edn., 2013, ch. 13.
- 72 L. Forlani, *J. Phys. Org. Chem.*, 1999, **12**, 417–424.
- 73 R. I. Cattana, J. O. Singh, J. D. Anunziata and J. J. Silber, *J. Chem. Soc., Perkin Trans. 2*, 1987, 79–83.
- 74 L. Forlani and V. Tortelli, *J. Chem. Res., Synop.*, 1982, **62**, 258–259.
- 75 I.-H. Um, S.-W. Min and J. M. Dust, *J. Org. Chem.*, 2007, **72**, 8797–8803.
- 76 E.-X. Zhang, D.-X. Wang, Q.-Y. Zheng and M.-X. Wang, *Org. Lett.*, 2008, **10**, 2565–2568.
- 77 N. H. Werstiuk and C. Ju, *Can. J. Chem.*, 1989, **67**, 5–10.
- 78 B. Yao, D.-X. Wang, H.-Y. Gong, Z.-T. Huang and M.-X. Wang, *J. Org. Chem.*, 2009, **74**, 5361–5368.
- 79 M.-J. Huang, S.-A. Hua, M.-D. Fu, G.-C. Huang, C. Yin, C.-H. Ko, C.-K. Kuo, C.-H. Hsu, G.-H. Lee, K.-Y. Ho, C.-H. Wang, Y.-W. Yang, I.-C. Chen, S.-M. Peng and C. Chen, *Chem. - Eur. J.*, 2014, **20**, 4526–4531.
- 80 F. A. Cotton, L. M. Daniels, C. A. Murillo, I. Pascual, H.-C. Zhou, *J. Am. Chem. Soc.* 1999, **121**, 6856–6861.
- 81 A.-L. Barra, F. Bianchi, A. Caneschi, A. Cornia, D. Gatteschi, L. Gorini, L. Gregoli, M. Maffini, F. Parenti, R. Sessoli, L. Sorace, A. M. Talarico, *Eur. J. Inorg. Chem.* 2007, 4145–4152.
- 82 J. Sandström, *Dynamic NMR Spectroscopy*, Academic Press, London, 1982.

## Table of Contents

The string-like Single Molecule Magnet  $[\text{Cr}_5(\text{tpda})_4\text{Cl}_2]$  features an alternation of Cr-Cr distances in its ground state, but solution NMR spectroscopy on  $^2\text{H}$  labelled samples unveils a  $D_4$  symmetric molecule, implying fast shuttling between the two unsymmetric configurations over NMR timescale.



# Solution Structure of a Pentachromium(II) Single Molecule Magnet from Isotopic Labelling and Multinuclear NMR Spectroscopy

Aivaras Dirvanauskas,<sup>a,b</sup> Rita Galavotti,<sup>a</sup> Alessandro Lunghi,<sup>‡c</sup> Alessio Nicolini,<sup>a</sup> Fabrizio Roncaglia,<sup>a</sup> Federico Totti<sup>c</sup> and Andrea Cornia<sup>a\*</sup>

<sup>a</sup>Department of Chemical and Geological Sciences, University of Modena and Reggio Emilia & INSTM, I-41125 Modena, Italy

<sup>b</sup>Department of Chemistry, University of Warwick, Gibbet Hill, Coventry, CV4 7AL, United Kingdom

<sup>c</sup>Department of Chemistry ‘Ugo Schiff’, University of Florence & INSTM, I-50019 Sesto Fiorentino (FI), Italy

<sup>‡</sup>Current address: School of Physics, AMBER and CRANN, Trinity College, Dublin 2, Ireland.

## Electronic Supplementary Information

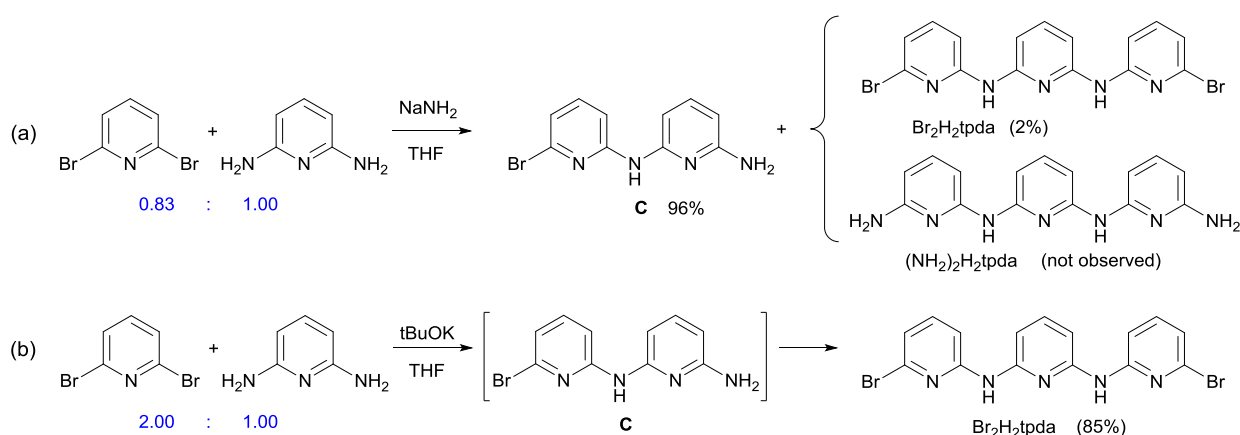


**Figure S1.** Reactivity of mixtures of 2,6-dibromopyridine and 2,6-diaminopyridine. In reaction (a),<sup>1</sup> an understoichiometric amount of 2,6-dibromopyridine affords very high yields of **C** but no  $(\text{NH}_2)_2\text{H}_2\text{tpda}$  as a consequence of the low electrophilicity of **C**. In reaction (b),<sup>2</sup> a 2:1 ratio of the reactants gives  $\text{Br}_2\text{H}_2\text{tpda}$  in high yields owing to the high nucleophilicity of **C**. The dibromide  $\text{Br}_2\text{H}_2\text{tpda}$  is formed only in trace amounts in reaction (a).  $\text{Br}_2\text{H}_2\text{tpda}$  could in principle be converted to  $\text{H}_2\text{tpda}$  through metal-catalyzed hydro-dehalogenation.<sup>3</sup>

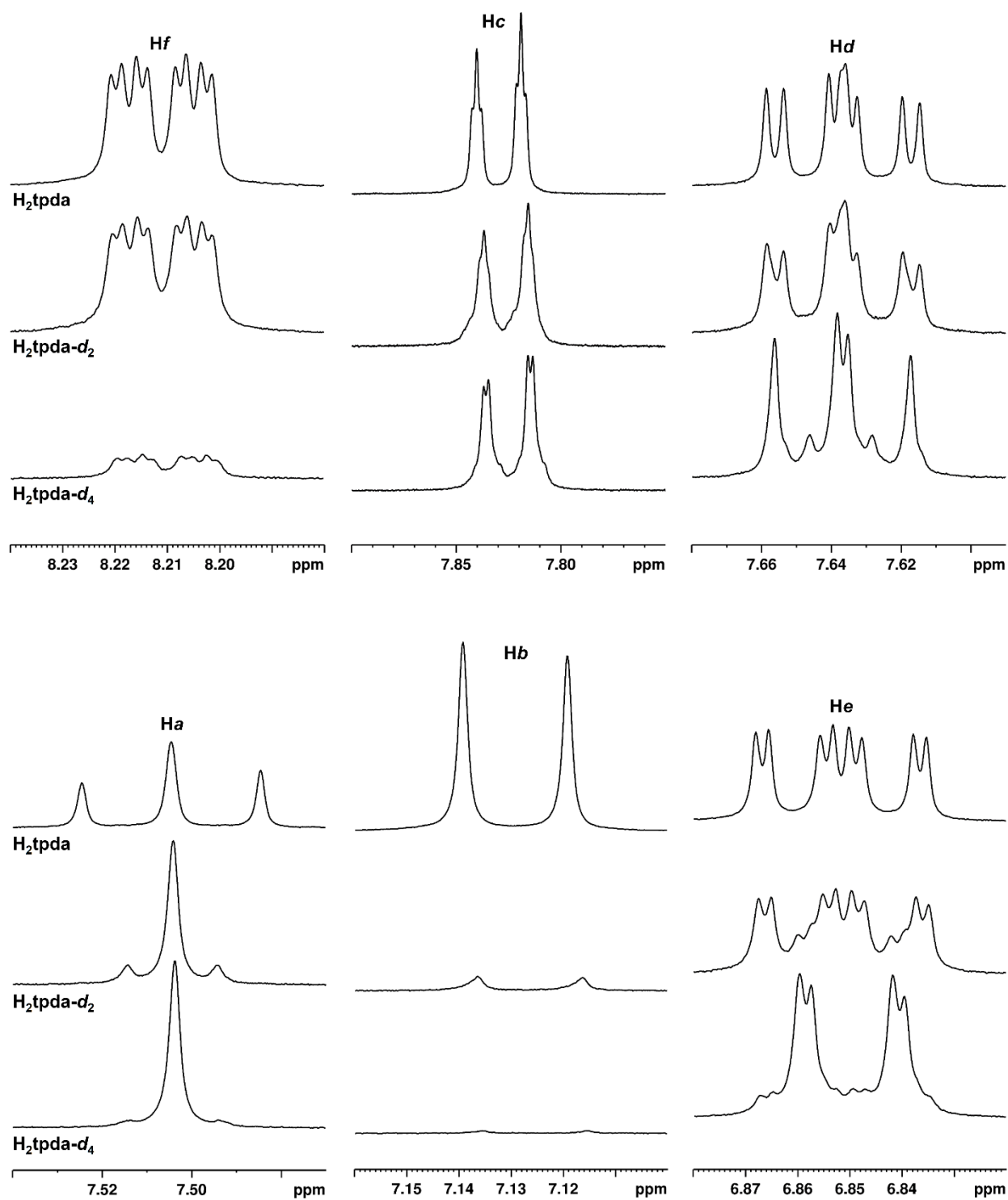


**Figure S2.** Scale-expanded proton NMR spectra of  $\text{H}_2\text{tpda}$ ,  $\text{H}_2\text{tpda}-d_2$ , and  $\text{H}_2\text{tpda}-d_4$  (solvent =  $\text{DMSO}-d_6$ ). For the labelling scheme, see Scheme 1.

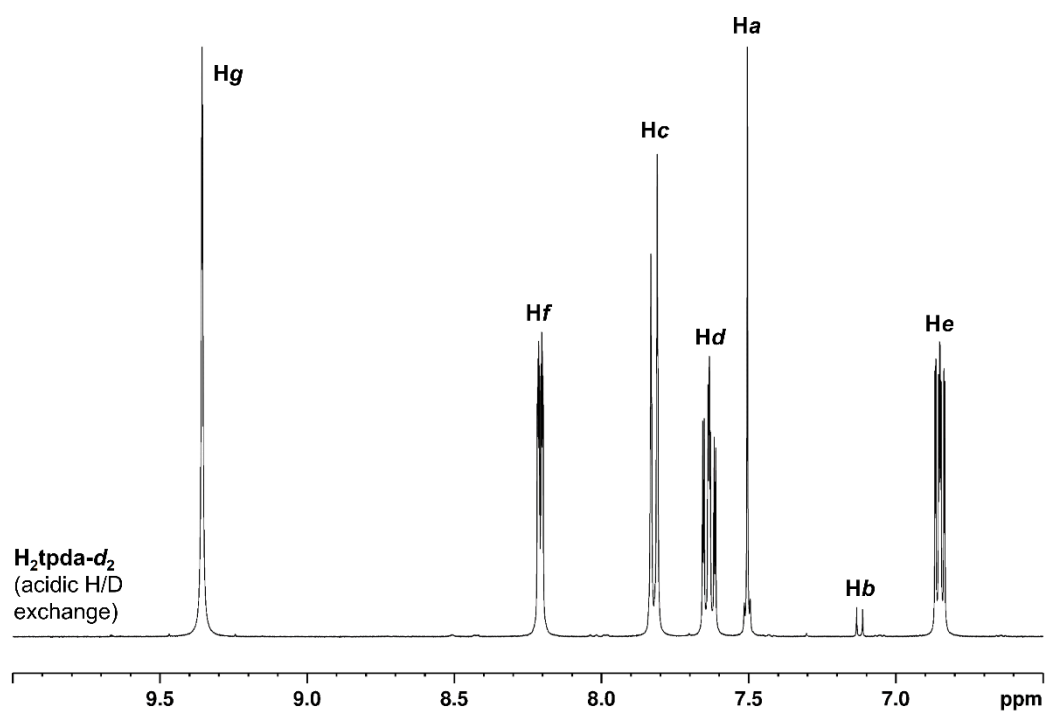


**Figure S3.** Proton NMR spectrum of H<sub>2</sub>tpda-*d*<sub>2</sub> obtained by acidic H/D exchange (solvent = DMSO-*d*<sub>6</sub>). For the labelling scheme, see Scheme 1.

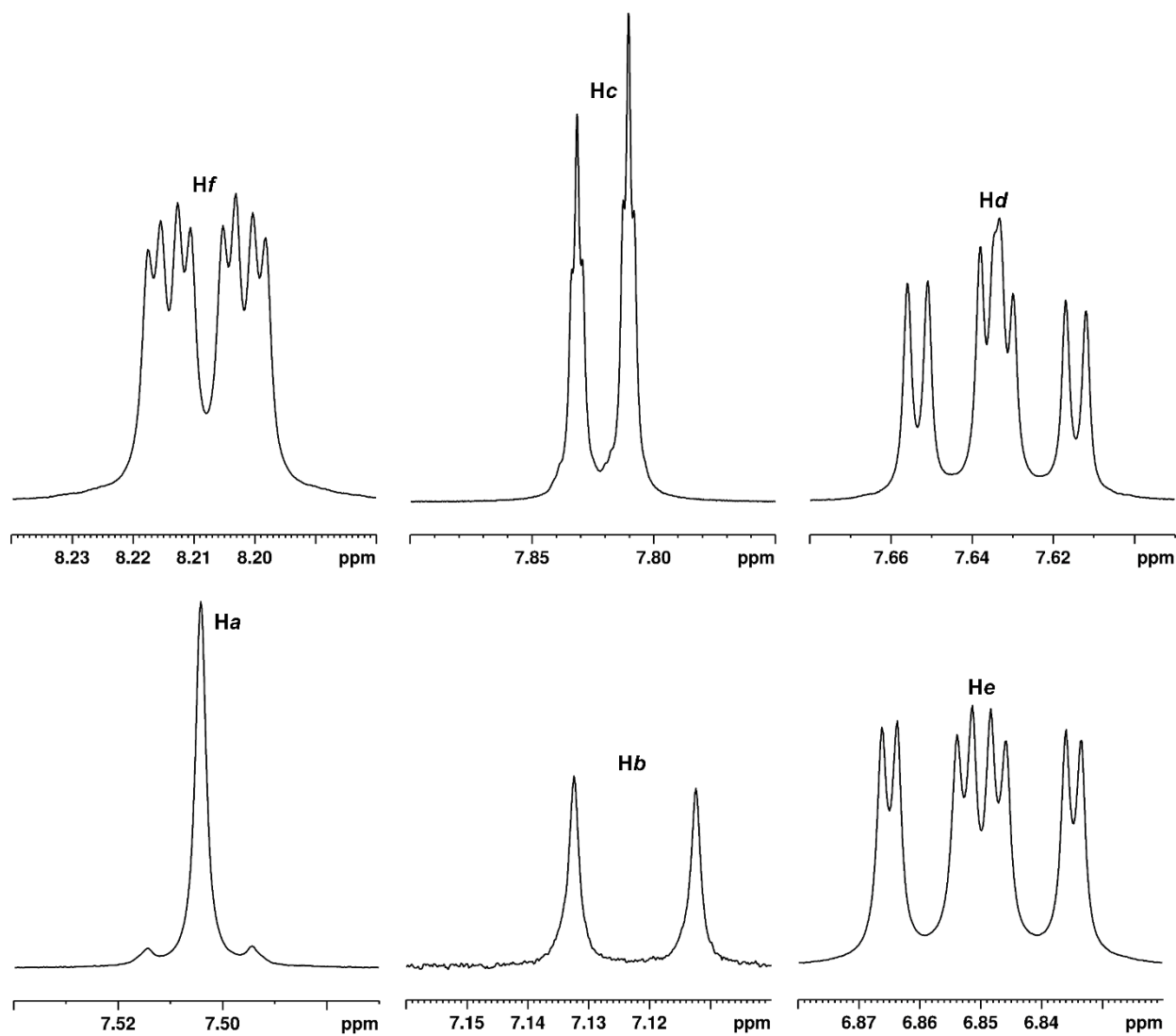


**Figure S4.** Scale-expanded proton NMR spectra of  $\text{H}_2\text{tpda-}d_2$  obtained by acidic H/D exchange (solvent =  $\text{DMSO-}d_6$ ). For the labelling scheme, see Scheme 1.



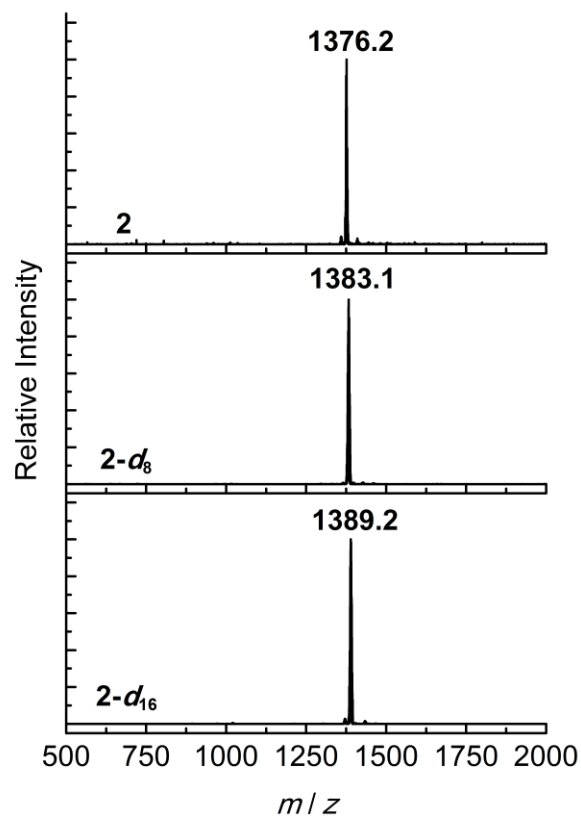


**Figure S5.** Full-range ESI-MS spectra of **2**, **2-d<sub>8</sub>** and **2-d<sub>16</sub>** (direct infusion, CH<sub>2</sub>Cl<sub>2</sub>, positive ion mode).

- 1 H. Hasan, U.-K. Tan, Y.-S. Lin, C.-C. Lee, G.-H. Lee, T.-W. Lin and S.-M. Peng, *Inorg. Chim. Acta*, 2003, **351**, 369–378.
- 2 H.-Y. Gong, X.-H. Zhang, D.-X. Wang, H.-W. Ma, Q.-Y. Zheng and M.-X. Wang, *Chem. - Eur. J.*, 2006, **12**, 9262–9275.
- 3 E.-X. Zhang, D.-X. Wang, Q.-Y. Zheng and M.-X. Wang, *Org. Lett.*, 2008, **10**, 2565–2568.